

Chapitre 3. Recent anthropogenic and climatic history of Nunatsiavut fjords (Labrador, Canada).

Résumé

Le but de cette étude est de reconstituer les conditions climatiques et environnementales récentes d'une région subarctique peu connue du Nord du Labrador : le Nunatsiavut. Une approche multi-*proxies* a été choisie, utilisant les assemblages fossiles de kystes de dinoflagellés, de diatomées et de pollen de séquences sédimentaires prélevées dans trois fjords (Nachvak 59°N; Saglek 58.5°N; Anaktalak 56.5°N). L'analyse palynologique des séquences sédimentaires, et les informations recueillies à partir des diatomées fossiles, ont permis d'estimer l'importance des influences terrestres et marines dans chacun des fjords et documenter les activités humaines récentes dans les fjords du sud (Saglek et Anaktalak). Les assemblages fossiles de pollens et de kystes de dinoflagellés permettent de décrire l'histoire climatique de la région au cours des derniers ~200-300 ans. Contrairement à la tendance générale au réchauffement observée dans les régions arctiques et subarctiques du Canada depuis le début de l'Ère Industrielle, le Nunatsiavut a connu une relative stabilité climatique au cours de cette période. Les assemblages fossiles de pollen documentent un déplacement de la limite des arbres vers le sud, illustrant le refroidissement des conditions terrestres. Nos reconstitutions suggèrent une grande stabilité climatique du Labrador au cours des derniers ~150-300 ans, accompagné d'une légère tendance au refroidissement des températures des eaux de surface inferrées perceptible dans les fjords de Saglek et Anaktalak.

Abstract

This study aimed at reconstructing past climatic and environmental conditions of a poorly known and documented subarctic region, the Nunatsiavut (northern Labrador). A multi-proxy approach was chosen, using fossil dinoflagellate cysts, diatoms and pollen from sediment cores taken into three fjords (Nachvak 59°N; Saglek 58.5°N; Anaktalak 56.5°N). It allowed estimating terrestrial and marine influences in each fjord and documenting the recent history of human activities of the southern fjords (Saglek and Anaktalak). Fossil pollen and dinoflagellate cyst assemblages allowed depicting the climate history of the region over the last ~200-300 years. In contrast to the general warming trend observed in the Arctic and sub-Arctic Canada since the beginning of the Industrial Era, the Nunatsiavut has experienced relative climate stability over this period. Fossil pollen data show a shift of the tree limit to the south illustrating the cooling of terrestrial conditions. Our reconstructions suggest that the Labrador region has remained climatically stable over the last ~150-300 years, with just a slight cooling trend of the reconstructed sea-surface temperatures, only perceptible in Saglek and Anaktalak fjords.

3.1. Introduction

Over the last 20 years, climate change has become a growing concern, not only in the scientific community, but also to public and policy makers (<http://www.ipcc.ch>). In order to understand mechanisms behind these changes, we first need to understand the natural variability of climate systems. Through a more detailed knowledge of the past, we intend to generate a better understanding of present-day conditions as well as to predict the future response of ecosystems and landscapes. Thus, the scientific community has developed tools to indirectly reconstruct past climatic and environmental conditions. Because the Arctic and sub-Arctic regions are anticipated to be most sensitive and affected by human-induced climate changes, several studies have been designed to document their past climatic history (ACIA, 2005; IPCC, 2007; AMAP, 2011).

As part of the ArcticNet project “Nunatsiavut Nuluak” (Richerol et al., 2012), our study aimed at reconstructing the past climatic history of a poorly studied sub-Arctic region in Labrador, specifically the Nunatsiavut (Figure 3.1). Among the few previous studies, some used fossil pollen and spore assemblages to reconstruct the evolution of terrestrial vegetation (Short and Nichols, 1977; Lamb, 1980; Vilks and Mudie, 1983; Lamb, 1984; Engstrom and Hansen, 1985; Viau and Gajewski, 2009), whereas other used fossil diatoms, chironomids or pollen and spores from lake sediment (Laing et al., 2002; Fallu et al., 2002, 2005; Smol et al., 2005; Gauthier, 2013) and other were based on the growth of tree rings (D’Arrigo et al., 1996, 2003). In some cases, these studies involved a multi-proxy approach, comparing terrestrial and marine records using fossil pollen and spores with fossil dinoflagellate cyst (= dinocyst) assemblages (Levac and de Vernal, 1997; Sawada et al., 1999). These studies evidenced a region dominated by relatively stable climatic conditions over at least the last ~5,000 years, with a slight cooling trend over the last ~200 years, which contrasts with the global warming recently observed in the rest of the Arctic and sub-Arctic regions (ACIA, 2005; Smol et al., 2005; PAGES 2k Consortium, 2013).

Our main objectives were to reconstruct past climatic conditions of the Nunatsiavut using a multi-proxy approach, and to use fossil pollen and spores, dinocyst and diatom assemblages from three marine sediment cores so as to better understand the recent climate history of the Nunatsiavut.

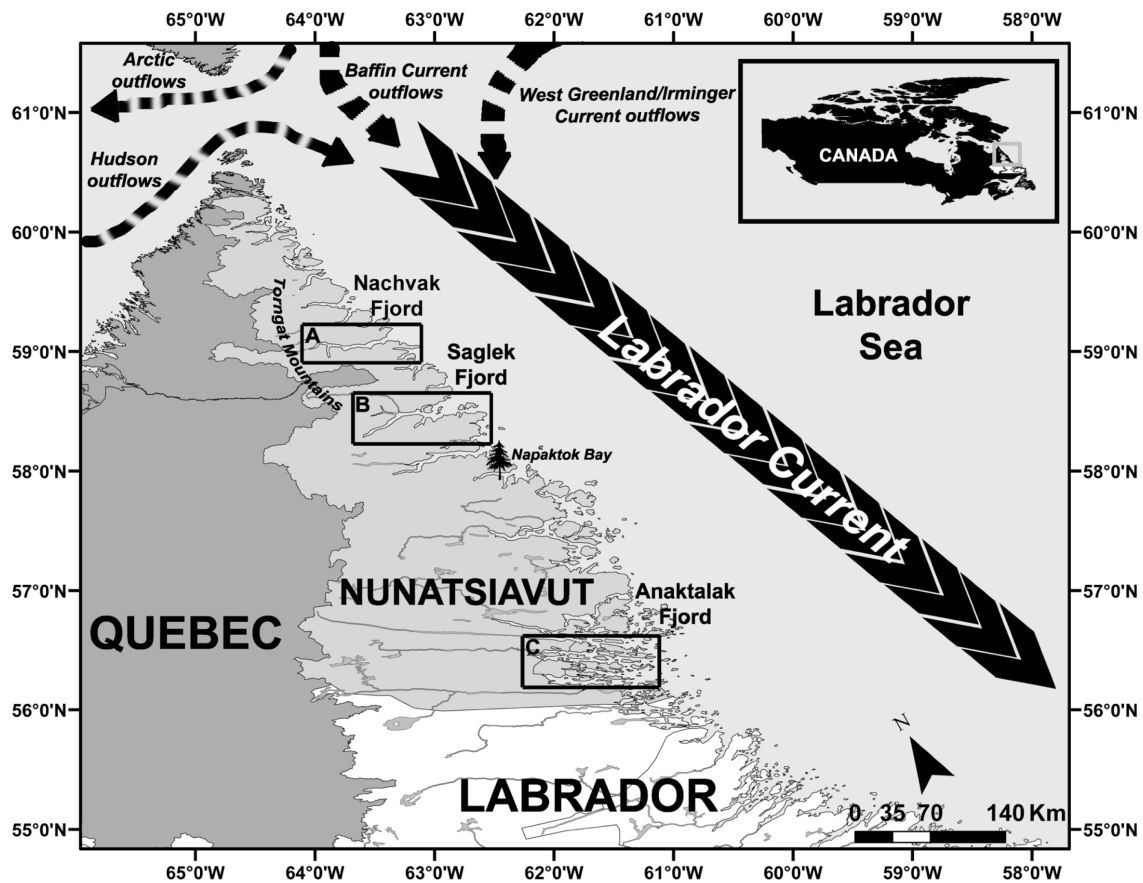


Figure 3.1 : Map of the Nunatsiavut (North Labrador, Canada) illustrating the location of the three fjords involved in this study: A. Nachvak Fjord; B. Saglek Fjord and C. Anaktalak Fjord and the nearby sea-surface circulation pattern in the Labrador Sea (modified from Richerol et al., 2012).

3.2. Environmental Settings

Labrador is a region located on the Canadian eastern seaboard and extends between 46 and 60° North along the Labrador Sea (Figure 3.1). Our study area is located in the northern part of the provinces of Newfoundland and Labrador that belong to the native Labradorian Inuit, also called the Nunatsiavut. Geological, oceanographical and climatological characteristics of the region, including its fjords, are summarized in Richerol et al. (2012). During the last Wisconsinan glaciation, the Laurentide Ice Sheet covered the entire region, which was carved by Pleistocene and Holocene glaciers into the high-relief landscape evident today, with the highest relief and only existing alpine glaciers in eastern mainland North America (Wilton, 1996; Bell et al., 2009; Bentley and Kahlmeyer, 2012). The Nunatsiavut is part of the tundra, more specifically the alpine tundra (Nachvak and Saglek) and the high subarctic forest-tundra (Anaktalak) (Fallu et al., 2002; Roberts et al., 2006). The northern tree limit on the Labrador coast is at Napaktok Bay (57°57'N, 62°30'W) (Figure 3.1), just south of Saglek Fjord (Elliot and Short, 1979). The northern forests of Labrador could have reached their environmental limit, as opposed to their climatic limit, as the valley landscape of Labrador has blocked any further movement north (Hare, 1951, 1976). North of 56°N, the black spruce (*Picea mariana*) is the most common tree species, along with some white spruce (*Picea glauca*) and eastern larch (*Larix laricina*). The vegetation of the tundra is also composed of dwarf shrubs (*Betula papyrifera*, *B. glandulosa*, *Alnus crispa* and 23 species of willow (*Salix* spp.)), graminoids, herbs, mosses and lichens (Lamb, 1984; Fallu et al., 2002; Roberts et al., 2006).

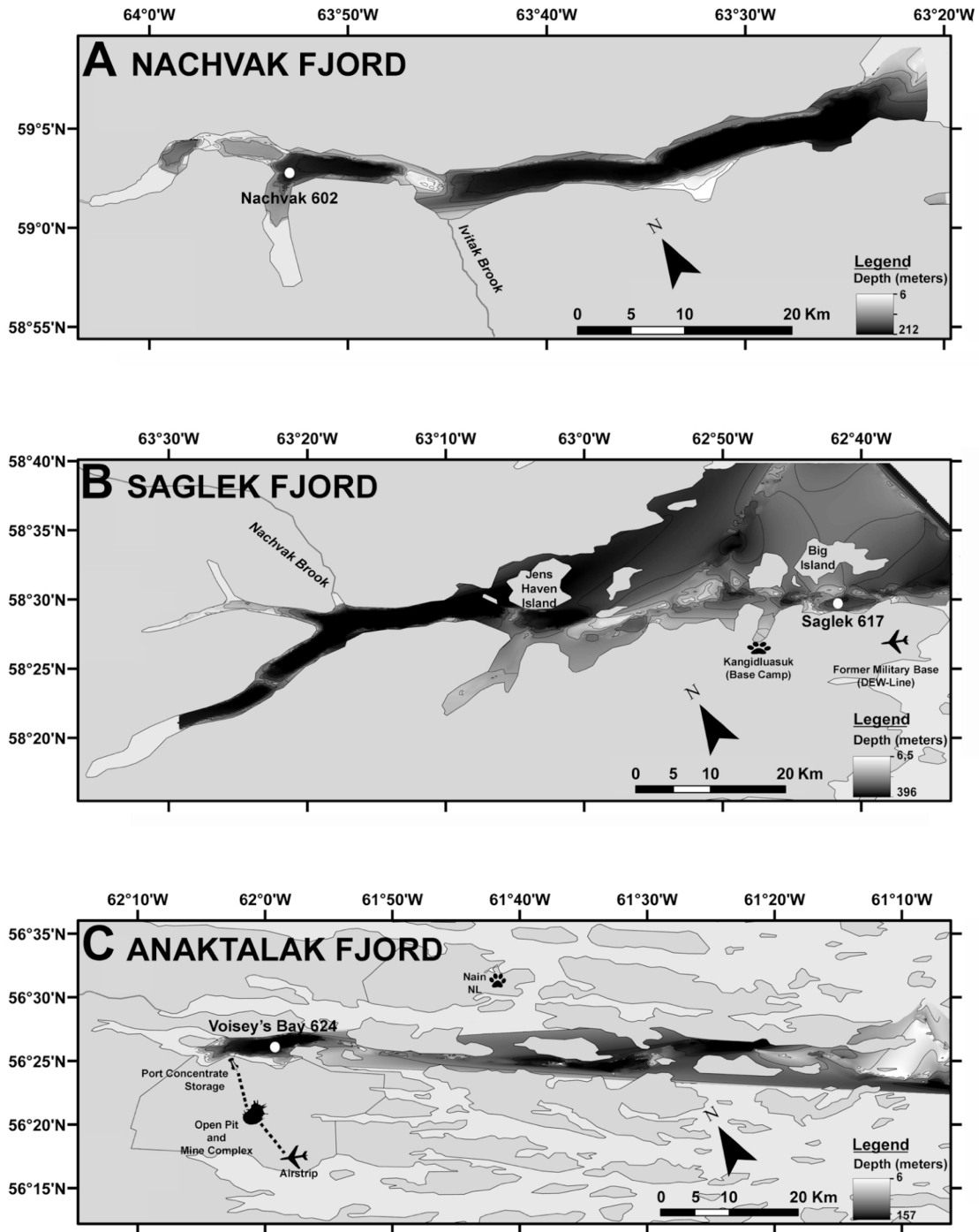


Figure 3.2 : Detailed maps of the three fjords showing the precise location of the three studied cores (modified from Richerol et al., 2012).

Nachvak is the northernmost studied fjord (Figures 3.1 and 3.2A), located in the Torngat Mountains National Park Reserve; hence it is the most remote and pristine system. This fjord serves as a reference or control site to assess natural climatic and environmental variability of the Labrador fjord ecosystems. Nachvak Fjord is 45 km long and 2 to 4 km wide, gradually increasing in width eastward to Nachvak Bay, which opens to the Labrador Sea. Local elevations extend up to 1,000 m above sea level (Bell and Josenhans, 1997). There is a succession of fjord basins with maximum water depths of 90, 160, 170, and 210 m from west to east. The four basins are separated by sills ranging between 10 and 180 m below sea level. Nachvak Fjord receives most of its sediments from Ivitak Brook, a glaciated catchment. The average annual sediment transport rate for the basins ranges between 1.1 to 3.2 kg s⁻¹ (Kahlmeyer, 2009; Bentley and Kahlmeyer, 2012).

Saglek Bay (Figures 3.1 and 3.2B) has been subject to PCB (PolyChloroBiphenyl) contamination from a nearby military radar station (Richerol et al., 2012). Saglek Fjord is unglaciated, 55 km long and 2 to 14 km wide, increasing in width eastward to Saglek Bay, which opens to the Labrador Sea. The sidewalls are generally steep, extending to more than 800 m above sea level. There is a succession of seven fjord basins with maximum water depths of 170, 256, 190, 117, 112, 149, and 160 m from west to east. The basins are separated by sills ranging between 45 and 96 m below sea level. Saglek Fjord receives the greatest amount of its sediments from Nachvak Brook, an unglaciated catchment. The average annual sediment transport rate for the basins ranges between 0.5 to 12 kg s⁻¹ (Kahlmeyer, 2009; Bentley and Kahlmeyer, 2012).

Voisey's Bay is the southernmost site and is located in Anaktalak Fjord (Figures 3.1 and 3.2C). This fjord is 66 km long and 1 to 5 km wide, gradually increasing in width eastward to the Labrador Sea. There are numerous islands of varying size within the fjord. Much of the bay forms a large basin of 100-120 m water depth. The depth rises to 85 m to form a sill at the outer part of the bay. The average sediment load entering the Voisey's Bay marine basin ranges from 0.04 to 0.45 kg s⁻¹ (Kahlmeyer, 2009). Since the beginning of the Vale Inco Nickel Mine

(formerly Voisey's Bay Nickel Company) operations, the fjord and marine environment have been transformed by the excavation and digging for the settlement (the port, the mine and the airstrip: Figure 3.2C) and the treated effluents they received from the mine (Hulett and Dwyer, 2003; Noble and Bronson, 2005; Richerol et al., 2012). The mine uses hydrometallurgy technology to reduce the impact on the environment by producing solid residues more manageable as opposed to smelting which releases sulphur dioxide and harmful dust particles (Dutrizac and Kuiper, 2006; Steel et al., 2009). However, there could be some risk of sulfuric acid production as a byproduct (Steel et al., 2010).

3.3. Methodology

3.3.1. Sampling process

Sampling in the Nunatsiavut fjords was carried out in November 2006 during leg 2 of the ArcticNet campaign onboard CCGS Amundsen. Three sedimentary sequences were collected in three fjords using PVC tubes with two diameters (7 and 10 cm) inserted into box cores (Table 3.1). Box-core N602-1 was collected in Nachvak Fjord (station 602), at the western end of the second inner basin of the fjord (Figure 3.2A). Box-core S617 was collected at the entrance of the Saglek Fjord (station 617). It is located in a bay, next to a former U.S. military base and its Long Range Radar Site (Figure 3.2B). Box-core V624 was retrieved in Anaktalak Fjord (station 624), in Edward's Cove, near the effluent from the Voisey's Bay mining site (Figure 3.2C). The three cores were described and then sampled at 1 cm or 2 cm intervals for the 10 cm-diameter or 7 cm-diameter cores for microfossil analyses, at the Laboratory of Marine Palynology, ISMER-UQAR (Rimouski, Québec). Grain-size and physical analyses (density, magnetic susceptibility, % organic matter, % water) were performed at 1 cm intervals for each core. A fraction of the sample (5 cm³) was dedicated to palynological analyses (dinocysts, pollen and spores, *Halodinium* sp., foraminifer linings and pre-Quaternary palynomorphs) using the standard method described by Rochon et al. (1999) and Richerol et al. (2008a,b). Another fraction of the sample (~1 cm³) was processed in the Aquatic Paleoecology Laboratory (LPA) at Laval University (Quebec) using the method of Scherer (1994) for the analysis of fossil diatom assemblages.

Table 3.1 : Details concerning the three studied cores: geographical coordinates, water depth, length and diameter of each core.

Fjord Name	Core Name	Latitude (°N)	Longitude (°W)	Water Depth (m)	Core Length (cm)	Core Diameter (cm)
Nachvak	N602-1	59.057	63.862	155	25	7
Saglek	S617	58.501	62.689	131	30	10
Anaktalak (Voisey's Bay)	V624	56.422	62.069	70	28	10

3.3.2. Sedimentological analysis

Grain-size analysis

The granulometric composition of each core was determined at 1 cm intervals using the laser granulometer Horiba® LA950v2. Samples were prepared following the protocol from the Laboratory of Geomorphology and Sedimentology at Laval University (Québec, QC). The free software Gradistat v4 (Blott and Pye, 2001) was used to statistically separate the different grain sizes and their percentages, as well as to calculate standard statistical parameters (mean, median and sorting) using the mathematical “method of moments” (Krumbein and Pettijohn, 1938).

Water content and Loss-On-Ignition (LOI)

The 1 cm-interval samples were weighed and then freeze-dried in order to determine water content percentages in sediments. A fraction of known weight of these dry samples was placed in a furnace at 550°C for 4h to determine percentages of organic matter in sediments (Heiri et al., 2001).

Using percentages of water and the organic matter content, we determined the dry bulk density (g cm^{-3}) and then the cumulative dry mass (g cm^{-2}) at each depth and for each core (Tables 3.2, 3.3, 3.4). The cumulative dry mass allows us to express a depth without taking into account the compaction effect (Appleby, 2001).

Table 3.2: Table showing dry bulk density (g cm^{-3}), cumulative dry mass (g cm^{-2}) and sedimentation rates ($\text{g cm}^{-2} \text{ year}^{-1}$ and cm year^{-1}) and their respective standard deviation (σ) for core N602-1. The italic lines represent depths for which sedimentation rates have been extrapolated.

Depth (cm)	Dry Bulk Density (g cm^{-3})	Cumulative Dry Mass (g cm^{-2})	Sedimentation Rate			
			$\text{g cm}^{-2} \text{ year}^{-1}$	σ	cm year^{-1}	σ
1.0	1.0097	1.0097	0.1429	0.0251	0.1415	0.0248
3.0	1.1334	3.1528	0.1429	0.0251	0.1260	0.0221
5.0	1.1010	5.3872	0.1429	0.0251	0.1298	0.0228
7.0	1.2412	7.7294	0.1429	0.0251	0.1151	0.0202
9.0	1.2078	10.1783	0.1429	0.0251	0.1183	0.0208
11.0	1.1729	12.5590	0.1429	0.0251	0.1218	0.0214
13.0	1.1965	14.9283	0.1429	0.0251	0.1194	0.0210
15.0	1.2598	17.3846	0.1429	0.0251	0.1134	0.0199
17.0	1.2764	19.9207	0.1429	0.0251	0.1119	0.0197
19.0	1.2610	22.4581	0.1429	0.0251	0.1133	0.0199
<i>21.0</i>	<i>1.3315</i>	<i>25.0506</i>	<i>0.1429</i>	<i>0.0251</i>	<i>0.1073</i>	<i>0.0188</i>
<i>23.0</i>	<i>1.3235</i>	<i>27.7056</i>	<i>0.1429</i>	<i>0.0251</i>	<i>0.1080</i>	<i>0.0190</i>
<i>24.5</i>	<i>1.1368</i>	<i>29.5507</i>	<i>0.1429</i>	<i>0.0251</i>	<i>0.1257</i>	<i>0.0221</i>

Table 3.3: Table showing dry bulk density (g cm^{-3}), cumulative dry mass (g cm^{-2}) and sedimentation rates ($\text{g cm}^{-2} \text{ year}^{-1}$ and cm year^{-1}) and their respective standard deviations (σ) for core S617. The italic lines represent depths for which sedimentation rates have been extrapolated.

Depth (cm)	Dry Bulk Density (g cm^{-3})	Cumulative Dry Mass (g cm^{-2})	Sedimentation Rate			
			$\text{g cm}^{-2} \text{ year}^{-1}$	σ	cm year^{-1}	σ
0.5	1.7145	0.8572	0.4989	0.0501	0.2910	0.0292
1.5	2.4584	2.9437	0.4550	0.0475	0.1851	0.0193
2.5	1.4569	4.9013	0.3644	0.0388	0.2501	0.0267
3.5	1.8951	6.5773	0.3327	0.0369	0.1755	0.0195
4.5	1.8533	8.4515	0.3677	0.0455	0.1984	0.0245
5.5	1.8096	10.2830	0.3716	0.0501	0.2054	0.0277
6.5	1.8747	12.1252	0.3404	0.0490	0.1816	0.0262
7.5	2.1782	14.1516	0.2446	0.0388	0.1123	0.0178
8.5	1.8728	16.1771	0.2693	0.0525	0.1438	0.0280
9.5	1.8893	18.0581	0.3118	0.0733	0.1650	0.0388
10.5	1.4746	19.7401	0.2371	0.0623	0.1608	0.0422
11.5	2.1051	21.5299	0.1893	0.0612	0.0899	0.0291
12.5	1.8450	23.5049	0.1627	0.0725	0.0882	0.0393
13.5	1.9797	25.4173	0.2270	0.1404	0.1146	0.0709
14.5	1.9226	27.3684	0.2462	0.1977	0.1281	0.1028
15.5	1.8876	29.2735	0.3028	0.3108	0.1604	0.1646
16.5	1.8649	31.1497	0.3539	0.4342	0.1898	0.2328
17.5	1.8821	33.0232	0.0609	0.1029	0.0323	0.0547
18.5	<i>1.6959</i>	<i>34.8122</i>	<i>0.1119</i>	<i>0.1209</i>	<i>0.0660</i>	<i>0.0713</i>
19.5	<i>1.5013</i>	<i>36.4109</i>	<i>0.1119</i>	<i>0.1209</i>	<i>0.0746</i>	<i>0.0805</i>
20.5	<i>1.4945</i>	<i>37.9088</i>	<i>0.1119</i>	<i>0.1209</i>	<i>0.0749</i>	<i>0.0809</i>
21.5	<i>1.5296</i>	<i>39.4209</i>	<i>0.1119</i>	<i>0.1209</i>	<i>0.0732</i>	<i>0.0790</i>
22.5	<i>1.6645</i>	<i>41.0179</i>	<i>0.1119</i>	<i>0.1209</i>	<i>0.0672</i>	<i>0.0726</i>
23.5	<i>1.5637</i>	<i>42.6320</i>	<i>0.1119</i>	<i>0.1209</i>	<i>0.0716</i>	<i>0.0773</i>
24.5	<i>1.7109</i>	<i>44.2693</i>	<i>0.1119</i>	<i>0.1209</i>	<i>0.0654</i>	<i>0.0707</i>
25.5	<i>1.9682</i>	<i>46.1088</i>	<i>0.1119</i>	<i>0.1209</i>	<i>0.0569</i>	<i>0.0614</i>
26.5	<i>1.8631</i>	<i>48.0245</i>	<i>0.1119</i>	<i>0.1209</i>	<i>0.0601</i>	<i>0.0649</i>
27.5	<i>1.9596</i>	<i>49.9358</i>	<i>0.1119</i>	<i>0.1209</i>	<i>0.0571</i>	<i>0.0617</i>
28.5	<i>2.1088</i>	<i>51.9700</i>	<i>0.1119</i>	<i>0.1209</i>	<i>0.0531</i>	<i>0.0573</i>
29.5	<i>1.8910</i>	<i>53.9699</i>	<i>0.1119</i>	<i>0.1209</i>	<i>0.0592</i>	<i>0.0639</i>

Table 3.4: Table showing dry bulk density (g cm^{-3}), cumulative dry mass (g cm^{-2}) and sedimentation rates ($\text{g cm}^{-2} \text{ year}^{-1}$ and cm year^{-1}) and their respective standard deviations (σ) for core V624. The italic lines represent depths for which sedimentation rates have been extrapolated.

Depth (cm)	Dry Bulk Density (g cm^{-3})	Cumulative Dry Mass (g cm^{-2})	Sedimentation Rate			
			$\text{g cm}^{-2} \text{ year}^{-1}$	σ	cm year^{-1}	σ
0.5	2.4517	1.2259	1.3445	0.0972	0.5484	0.0397
1.5	2.2793	3.5914	0.6631	0.0335	0.2909	0.0147
2.5	2.5385	6.0003	0.5747	0.0312	0.2264	0.0123
3.5	2.5701	8.5545	0.4369	0.0230	0.1700	0.0090
4.5	2.3256	11.0024	0.4856	0.0311	0.2088	0.0134
5.5	2.5911	13.4608	0.6002	0.0454	0.2316	0.0175
6.5	2.7496	16.1312	0.5335	0.0375	0.1940	0.0136
7.5	2.6741	18.8430	0.4083	0.0333	0.1527	0.0125
8.5	2.9687	21.6644	0.5778	0.0587	0.1946	0.0198
9.5	3.0939	24.6956	0.3748	0.0414	0.1212	0.0134
10.5	3.0662	27.7757	0.2823	0.0411	0.0921	0.0134
11.5	2.8215	30.7195	0.2181	0.0445	0.0773	0.0158
12.5	2.6898	33.4752	0.1852	0.0566	0.0689	0.0211
13.5	2.9736	36.3069	0.1375	0.0715	0.0462	0.0240
14.5	3.1707	39.3790	0.0593	0.0845	0.0187	0.0267
15.5	3.1497	42.5392	<i>0.1500</i>	<i>0.0643</i>	<i>0.0476</i>	<i>0.0204</i>
16.5	2.9613	45.5947	<i>0.1500</i>	<i>0.0643</i>	<i>0.0507</i>	<i>0.0217</i>
17.5	3.3870	48.7689	<i>0.1500</i>	<i>0.0643</i>	<i>0.0443</i>	<i>0.0190</i>
18.5	3.0560	51.9904	<i>0.1500</i>	<i>0.0643</i>	<i>0.0491</i>	<i>0.0210</i>
19.5	3.4274	55.2320	<i>0.1500</i>	<i>0.0643</i>	<i>0.0438</i>	<i>0.0188</i>
20.5	3.2782	58.5848	<i>0.1500</i>	<i>0.0643</i>	<i>0.0458</i>	<i>0.0196</i>
21.5	2.9101	61.6790	<i>0.1500</i>	<i>0.0643</i>	<i>0.0516</i>	<i>0.0221</i>
22.5	3.1157	64.6919	<i>0.1500</i>	<i>0.0643</i>	<i>0.0482</i>	<i>0.0206</i>
23.5	3.0295	67.7645	<i>0.1500</i>	<i>0.0643</i>	<i>0.0495</i>	<i>0.0212</i>
24.5	3.5489	71.0537	<i>0.1500</i>	<i>0.0643</i>	<i>0.0423</i>	<i>0.0181</i>
25.5	3.1754	74.4159	<i>0.1500</i>	<i>0.0643</i>	<i>0.0472</i>	<i>0.0202</i>
26.5	2.8900	77.4486	<i>0.1500</i>	<i>0.0643</i>	<i>0.0519</i>	<i>0.0222</i>
27.5	3.1022	80.4447	<i>0.1500</i>	<i>0.0643</i>	<i>0.0484</i>	<i>0.0207</i>

3.3.3. Chronological framework

Our chronology is mainly based on ^{210}Pb measurements. However, shell fragments found at two depths (23 cm and 24.5 cm) near the base of core S617 (30 cm length), enabled us to obtain AMS- ^{14}C (Accelerated Mass Spectrometry)

dates. The preparation of the samples was performed at the Radiochronology Laboratory of the Center for Northern Studies (Laval University, Québec, Canada) and the analyses at the Keck Carbon Cycle AMS Facility (Earth System Science department, University of California, Irvine, USA). Calibration of all AMS-¹⁴C dates in years A.D. (*Anno Domini*) was performed using the software CALIB 6.0 (Stuiver et al., 2005) associated with a marine reservoir correction (ΔR) of 227 ± 56 years based on the two closest sites (Fish Island, Labrador : 58.35°N , 62.45°W ; Hebron Fjord, Labrador : 58.20°N , 62.63°W). The obtained calibrated dates were 1786 ± 120 years A.D. (23 cm) and 1680 ± 154 years A.D. (24.5 cm).

Measurements of ²¹⁰Pb total activity (in dpm g⁻¹ for disintegrations per minute) were performed at the GEOTOP (UQAM – Montréal, Canada) on the uppermost 20 cm of each sediment core and transformed in Bq g⁻¹ (Becquerel; 1 Bq=60 dpm). By plotting the ²¹⁰Pb total activity against the cumulative dry mass, we were able to determine an approximate value for the natural supported ²¹⁰Pb activity for each core. Thus, we deduced the unsupported ²¹⁰Pb and plotted its natural logarithm trend against the cumulative dry mass. Using the shape of the curve (Appleby and Oldfield, 1983; Oldfield and Appleby, 1984; Sorgente et al., 1999; Appleby, 2001), we were able to decide which model to apply to estimate a sedimentation rate and develop an age model for each core. These model consist in CF-CS (Constant Flux – Constant Sedimentation : sedimentation rate and ²¹⁰Pb flux are constants), CIC (Constant Initial Concentration : sedimentation rate and ²¹⁰Pb flux vary simultaneously) and CRS (Constant Rate of Supply : sedimentation rate varies, ²¹⁰Pb flux is constant).

3.3.4. Palynomorphs preparations

Preparation of fossil palynomorphs (dinocysts, pollen and spores, acritarchs, freshwater palynomorphs) followed standard procedures as outlined in Richerol et al. (2008a,b, 2012).

Palynomorphs were counted using a transmitted-light microscope (Leica DM 5500B) with a magnification factor of 400× at Aquatic Paleoecology Laboratory (Laval University, Québec, Canada). A minimum of 300 dinocysts were counted in each sample, as this method yielded the best statistical representation of all taxa present in the samples. The nomenclature used for the identification of dinocysts corresponds to Rochon et al. (1999), Head et al. (2001), the index of Lentin and Williams (Fensome and Williams, 2004) and Radi et al. (2013). The nomenclature used for the identification of pollen grains and spores followed McAndrews et al. (1973).

Studies from Zonneveld et al. (1997, 2001) and Zonneveld and Brummer (2000) have shown species sensitivity to oxygen availability. Especially cysts from the *Protoperidinium* group, such as *Brigantedinium* spp., are the most sensitive species, followed by the genus *Spiniferites*, *Impagidinium* and *Operculodinium*. High sedimentation rates measured in Nunatsiavut fjords prevent the dinocyst assemblages from oxidation. As a consequence, the most sensitive taxa, such as *Brigantedinium* spp., showed excellent preservation with the operculum still attached on many specimens.

3.3.5. Statistical analysis

Biozonation through clustering

In order to statistically determine dinocyst and pollen assemblage zones, the software “R” was used in combination with the libraries “vegan” and “rioja” to produce a cluster showing the Euclidean distance between each sample for each core. Using the “decostand” function, the relative abundances of all taxa were standardized and the resulting matrix was transformed into a Euclidean distance matrix. The grouping test CONISS (Grimm, 1987) was then applied to the distance matrix using the “chclust” function (Borcard et al., 2011). A hierarchical clustering was obtained for each core according to the depth.

Dinocyst-based quantitative reconstructions

In order to validate the addition of our twelve modern dinocyst assemblages from Nunatsiavut (Richerol et al., 2012) to the GEOTOP (Research Center in Geochemistry and Geodynamic) database (N = 1,429), it is mandatory to determine the range of the standard deviation of the reconstructions using the 'N = 1,441' database. For this purpose, we used the software "R" and the Modern Analogue Technique package (MAT). The new dinocyst database (N = 1,441) was artificially and randomly split into two parts (80/20) and a reconstruction was performed on the 20% part using the other 80% part as a reference database. Instrumental values of the reconstructed temperature, salinity, sea-ice cover duration and annual productivity from the database were compared to the reconstructed values of the same parameters. The linearity of the relationship between estimates and observations (R^2) provides a first indication of the performance and reliability of the transfer function. Moreover, we obtained a standard deviation value (RMSEP – Root Mean Square Error of Prediction) for each parameter that provides an estimation of the reliability of the reconstructions (Richerol et al., 2008b) (Figure 3.3).

The best reconstruction was obtained for August Sea Surface Temperature (SST) with a correlation coefficient of $R^2 = 0.95$ and a RMSEP of $\pm 1.72^\circ\text{C}$. August Sea Surface Salinity (SSS) exhibit a scattered distribution below 26 due to freshwater inputs from rivers and sea-ice melting (de Vernal et al., 2001; Richerol et al., 2008b; Bonnet et al., 2012), resulting in a $R^2 = 0.72$ and a RMSEP of ± 2.22 . Sea-ice reconstruction also shows a scattered distribution, which reflects its interannual variability, with a $R^2 = 0.86$ and a RMSEP of ± 1.33 months year⁻¹ (Figure 3.3). Validation tests were previously performed with 'N = 677' database (de Vernal et al., 2001), 'N = 1,171' database (Radi and de Vernal, 2008; Richerol et al., 2008b) and 'N = 1,419' (Bonnet et al., 2012) for the Northern Hemisphere. Overall, our results are similar. However, additional sites included in the database result in a higher variability in salinity and sea-ice cover, thus an increase in the

RMSEP. The annual productivity is not adequately reconstructed with a $R^2 = 0.80$ and a RMSEP of $\pm 61.27 \text{ g C m}^{-2} \text{ year}^{-1}$ (Figure 3.3), which is equivalent to the 'N = 1,419' database validation test for the annual productivity (Bonnet et al., 2012) but worse than the one for the 'N = 1,171' database (Radi and de Vernal, 2008). The complex nature of the fjords, the limited number of reference sites, and the ambiguous relationship between surface productivity and dinocyst assemblages could explain this lack of accuracy. Indeed, a recent study by Cormier (2013) in the northern Baffin Bay suggested that diatoms may be the major contributors to primary productivity over dinoflagellates in environments characterized by a stable sea-ice cover.

Reconstructions of sea-surface parameters were then performed with the software "R" using fossil dinocyst assemblages, the MAT transfer functions and the search for analogs in the updated dinocyst modern database ('N = 1,441') (Richerol et al., 2008b, 2012). Here we also used the "bioindic" package developed on the R-platform (<http://cran.r-project.org/>) which is especially devoted to provide various types of statistical analyses.

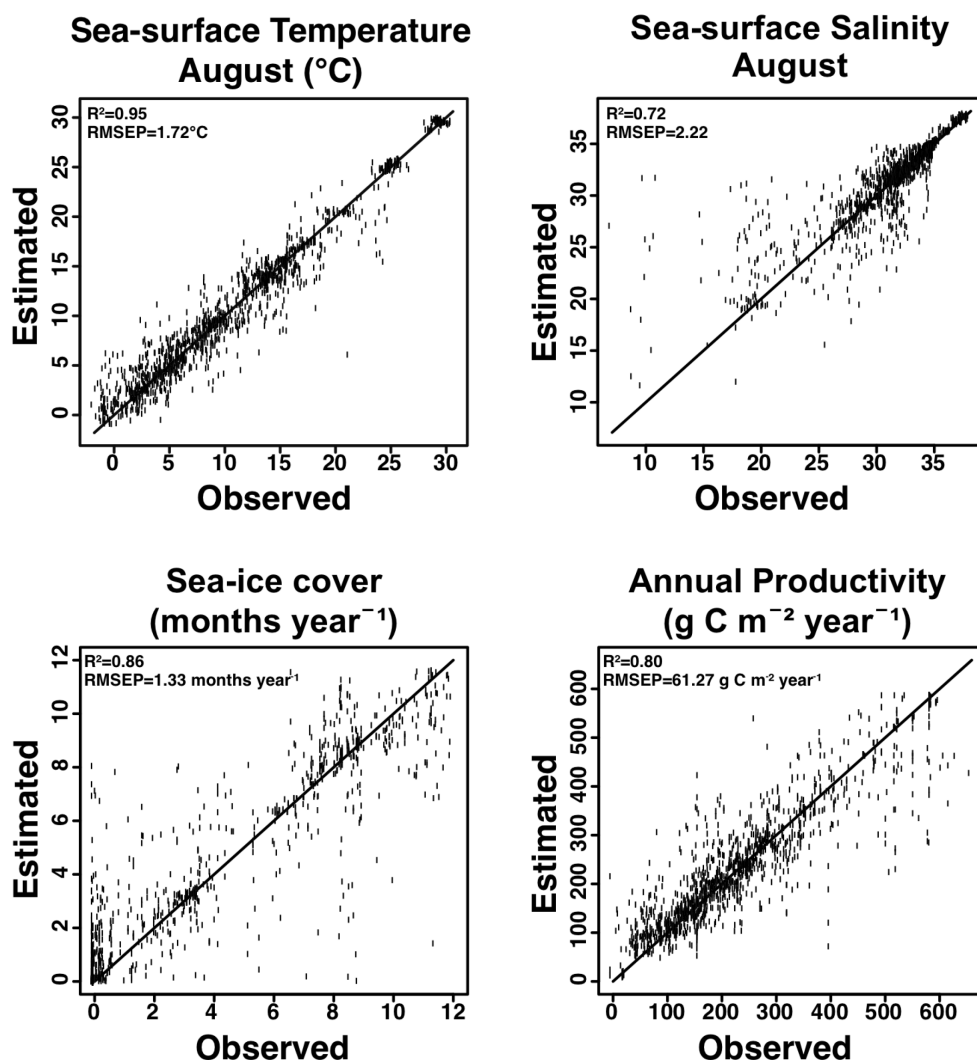


Figure 3.3 : Validation test of the 'N = 1,441' database for the four reconstructed parameters : August Sea-Surface Temperature (SST, in °C), August Sea-Surface Salinity (SSS), Sea-Ice Cover duration (months year⁻¹) and Annual Productivity (g C m⁻² year⁻¹). RMSEP = Root Mean Square Error of Prediction.

3.3.6. Diatom laboratory procedure

Preparation of fossil diatoms followed standard procedures as outlined in Scherer (1994). Approximately 1 g of sediment was taken from each sample and placed in a 20 mL identified glass vial. Samples were treated with hydrogen peroxide (30% H₂O₂) in order to dissolve organic matter.

Diatoms were counted using a transmitted-light microscope (Leica DM 5500B) with a magnification factor of 1000× at the Aquatic Paleoecology Laboratory (Laval University, Québec, Canada). A minimum of 500 diatom valves were counted in each sample, with a minimum of 100 microspheres. The nomenclature used for the identification of diatoms followed that presented in Campeau et al. (1999) and Fallu et al. (2000).

Diatom frustules were poorly preserved in our sediments. Most of the time, the identification was not possible beyond the genus level. Preservation problems are often encountered in coastal areas such as fjord systems, with semi-terrestrial conditions and reduced tidal influence (Sticklely et al., 2008; Stoermer and Smol, 1999).

3.4. Results

3.4.1. Chronological framework

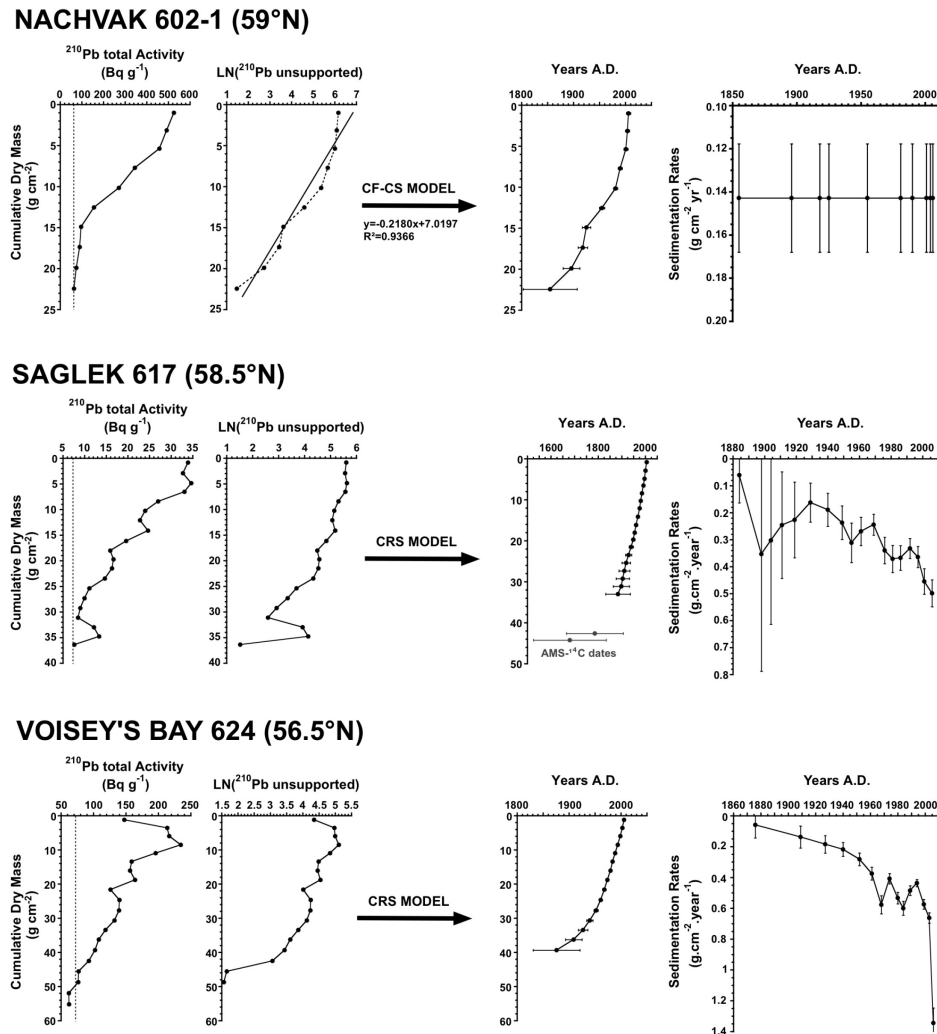


Figure 3.4 : ^{210}Pb profiles of the three cores used to establish sedimentation rates ($\text{g cm}^{-2} \text{ year}^{-1}$) and chronological frameworks (years A.D.). The curves of the ^{210}Pb total activity (Bq g^{-1}) and natural logarithm of the unsupported ^{210}Pb activity are represented according to the depth expressed as Cumulative Dry Mass (g cm^{-2}) in order to correct for sediment compaction. The vertical dotted line on the first graph represents the estimated value of the supported ^{210}Pb activity. Standard deviations for ages obtained are also depicted. Gray dots for Saglek 617 core represent the two AMS- ^{14}C dates obtained at the base of the core.

For N602-1 core, the shape of the natural logarithm of ^{210}Pb -unsupported is close to a straight line. As the station is located in a pristine fjord (Richerol et al., 2012), in a basin far inside the fjord (Figure 3.2A), we decided to apply the CF-CS model. Hence we estimated a constant sedimentation rate of $0.1429 \pm 0.0251 \text{ g cm}^{-2} \text{ year}^{-1}$. The age model deduced from this sedimentation rate spans the last 156 years down to 20 cm depth with a pluri-annual to decadal resolution (Figure 3.4). The sedimentation rate being constant, we were able to extrapolate, using the dry bulk density, an average sedimentation rate of $0.1136 \pm 0.02 \text{ cm year}^{-1}$ for the remaining depths between 20 and 25 cm (Table 3.2), until the base of the core.

Core S617 is located in a bay at the mouth of the fjord (Figure 3.2B), therefore more subject to changes in sedimentation dynamics. This latter fact as well as the shape of the natural logarithm ^{210}Pb -unsupported curve with peaks and troughs lead us to apply the CRS model (Figure 3.4). We then calculated a sedimentation rate in $\text{g cm}^{-2} \text{ year}^{-1}$ at each depth, and estimated a mean value of $0.1596 \pm 0.0552 \text{ cm year}^{-1}$. The age model deduced from this mean sedimentation rate spans the last 122 years down to 18 cm depth with a pluri-annual to decadal resolution (Figure 3.4). The two additional AMS- ^{14}C dates at 23 cm and 24.5 cm allowed us to interpolate an average sedimentation rate of $0.1119 \pm 0.1209 \text{ g cm}^{-2} \text{ year}^{-1}$ between 18 and 25 cm and then to extrapolate this value until the base of the core (Table 3.3).

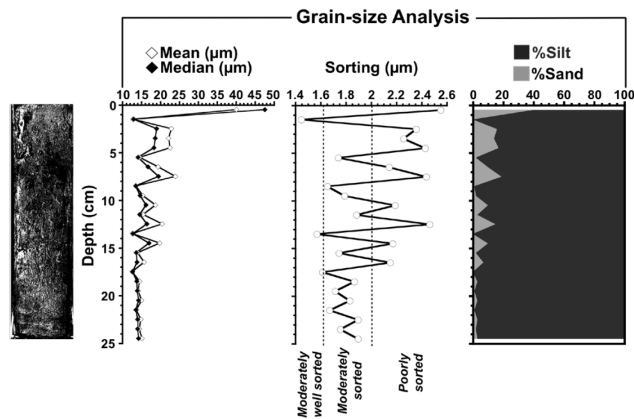
Core V624 is located in a bay in the fjord, near a recently installed mining complex (Richerol et al., 2012) (Figure 3.2C). This latter fact as well as the shape of the natural logarithm ^{210}Pb -unsupported curve with peaks and troughs lead us to apply the CRS model (Figure 3.4). We then calculated a sedimentation rate in $\text{g cm}^{-2} \text{ year}^{-1}$ at each depth, and estimated a mean value of $0.1761 \pm 0.0178 \text{ cm year}^{-1}$. The age model deduced from this sedimentation rate spans the last 130 years down to 15 cm depth with a pluri-annual to decadal resolution (Figure 3.4). Sedimentation rates show an important peak between 1990

and 2006 years A.D. (Figure 3.4). We used the four bottom values for sedimentation rate to extrapolate a mean sedimentation rate of $0.1500 \pm 0.0643 \text{ g cm}^{-2} \text{ year}^{-1}$ between 15 and 28 cm (Table 3.4). However, unlike N602-1 and S617 cores, we have chosen not to extrapolate the dates in year A.D. from 15 cm to the bottom of the core because of the large standard deviation for these four sedimentation rate values (Figure 3.4).

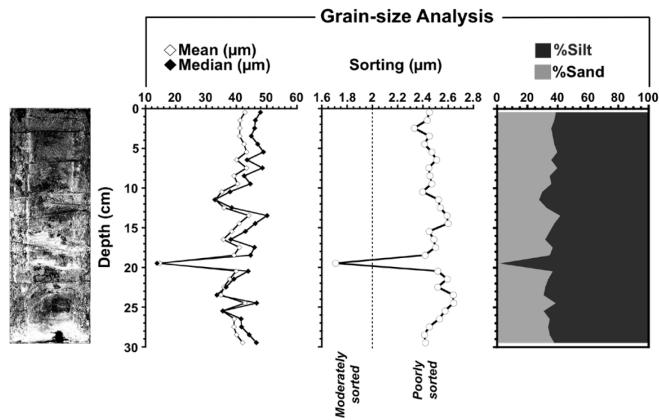
3.4.2. Sedimentology

For the three cores, mean and median grain sizes are included in the dominant mode of the silt and vary between $10 \mu\text{m}$ and $60 \mu\text{m}$ (Figure 3.5).

NACHVAK 602-1 (59°N)



SAGLEK 617 (58.5°N)



VOISEY'S BAY 624 (56.5°N)

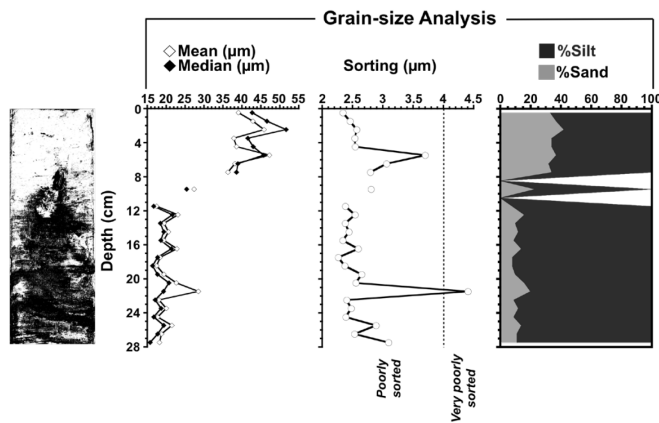


Figure 3.5 : Sedimentological analyses of the three cores represented in depth scale (cm). From left to right: gray-level picture for each core ; grain-size analysis (mean, median and sorting (μm)) and percentages of silt and sand. For V624 core, grain-size analysis is discontinuous at 8.5 cm and 10.5 cm due to flushing and loss of the corresponding samples in the laser grain-size analyzer.

Grain-size analyses acquired for the three cores generally showed a bimodal grain size distribution. We observe in each core a dominant silt fraction (> 60%) and a smaller sand fraction (< 40%) (Figure 3.5). Within the silt fraction, grain-size correspond to fine to very coarse silt (4 to 63 μm for N602-1 and V624) or medium to very coarse silt (8 to 63 μm for S617). Within the sand fraction, grain-size correspond to very fine to medium sand (63 to 500 μm for N602-1 and S617) or very fine to very coarse sand (63 μm to 2 mm for V624). We note, in V624, an occurrence of very fine gravel (2-4 mm) at 5.5 cm depth and of coarse sand (0.5-1 mm) at 21.5 cm depth.

The sorting (=standard deviation) spanned 1.4 to 4.5 μm with increasing sorting from north (1.4-2.6 μm) to south (2-4.5 μm) and is more variable in N602-1 core (Figure 3.5). For each core, mean and median grain size are coherently correlated with silt percentages, whereas sorting profiles coincide with sand percentages. When mean grain-size is higher than the median, a skewed distribution (dominance of fine material (Bouchard et al., 2011)) is illustrated (Figure 3.5).

Finally, we observe that sorting (Krumbein and Pettijohn, 1938; Blott and Pye, 2001) follows a north-south trend from moderately well sorted (N602-1) to very poorly sorted (V624) (Figure 3.5).

3.4.3. Palynomorph fluxes

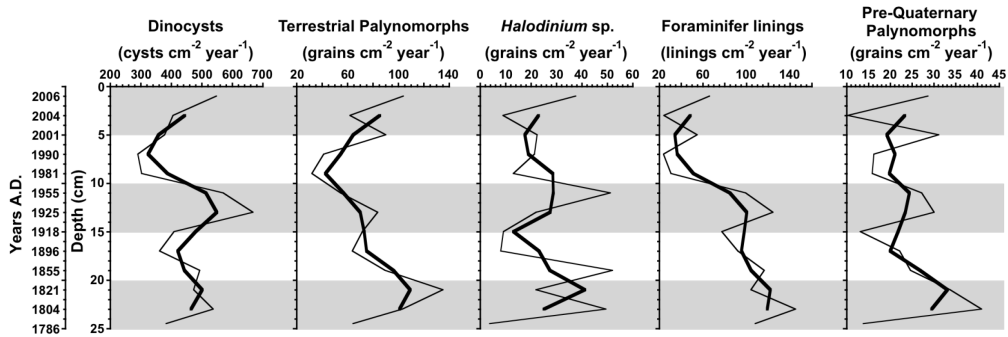
In addition to dinocysts, which are good indicators of planktonic productivity (Richerol et al., 2008b), we have identified and counted four other types of palynomorphs (Figure 3.6):

- *Halodinium* sp., an acritarch and freshwater tracer (e.g. Richerol et al., 2008b);

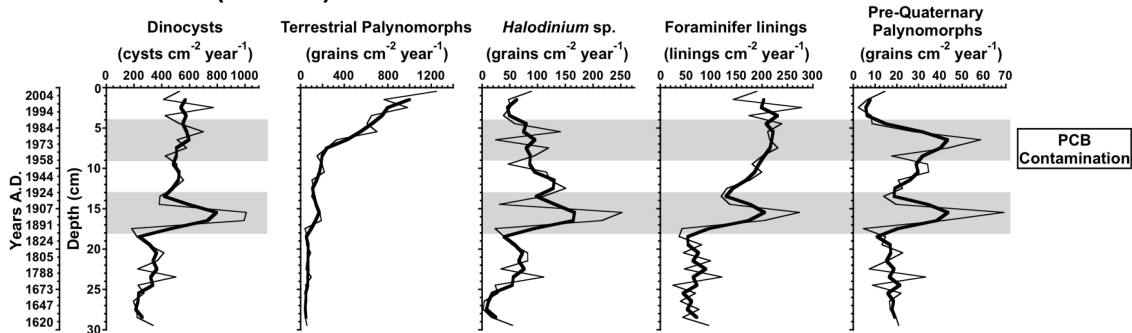
- terrestrial palynomorphs such as pollen grains and spores, which allow us to compare terrestrial *versus* marine climate changes (e.g. Richerol et al., 2008b);
- foraminifer linings, which are indicators of benthic marine productivity (e.g. de Vernal et al., 1992);
- pre-Quaternary palynomorphs, including dinocysts, acritarchs, pollen grains and spores, which are indicators of ancient and/or distant erosive material advection (e.g. de Vernal et Hillaire-Marcel, 1987; Durantou et al., 2012).

We have calculated palynomorphs fluxes (specimens $\text{cm}^{-2} \text{year}^{-1}$) using the sedimentation rates (cm year^{-1}), thus obtaining a better representation of their variations with regards to changes in sediment accumulation for each core (Figure 3.6). From North to South, we observe an increase of dinocyst, terrestrial palynomorph and foraminifer lining fluxes.

NACHVAK 602-1 (59°N)



SAGLEK 617 (58.5°N)



VOISEY'S BAY 624 (56.5°N)

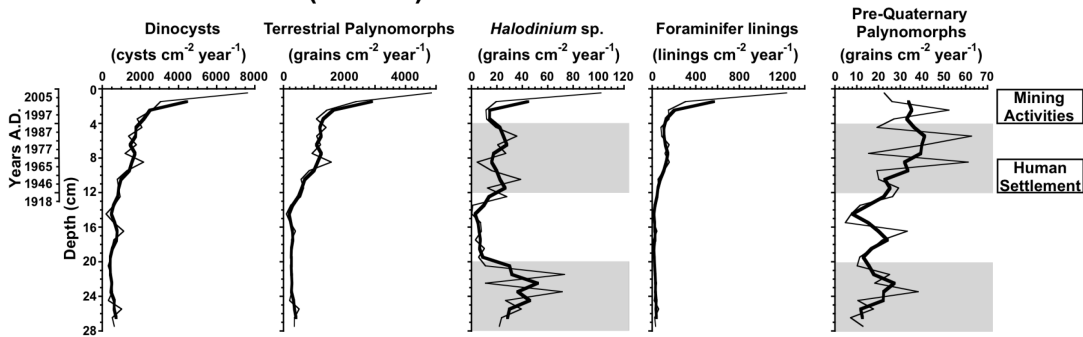


Figure 3.6 : Fluxes of the five types of palynomorphs counted, according to depth (cm) and time (years A.D.), for each sediment core : dinocysts (cysts cm⁻² year⁻¹), terrestrial palynomorphs (grains cm⁻² year⁻¹), *Halodinium* sp. (grains cm⁻² year⁻¹), foraminifer linings (linings cm⁻² year⁻¹) and pre-Quaternary palynomorphs (grains cm⁻² year⁻¹). For each curve, the black thick line is a smooth on three values. Gray areas highlight the major features presented in the result section.

In N602-1, all palynomorph fluxes show very similar profiles. They decrease gradually from the bottom to the top of the core in a series of oscillations. Especially, three peaks in all palynomorph fluxes are centered around 25-20 cm

(1786-1830 A.D.), 15-10 cm (1918-1968 A.D.) and 5 cm to the top (2001-2006 A.D.) (Figure 3.6).

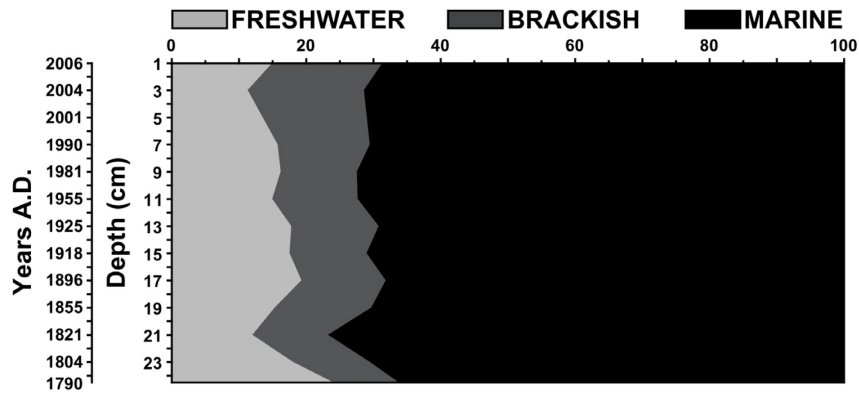
In S617, all palynomorph fluxes, with the exception of terrestrial palynomorphs, show a global similar trend, with relatively low and constant values from the base to 18 cm, followed by increasing values toward the top marked by major oscillations (18-13 cm (1857-1924 A.D.); 9-4 cm (1958-1989 A.D.)) (Figure 3.6). Terrestrial palynomorph fluxes remain relatively constant until 8 cm and increase steadily from 8 cm onwards.

In V624, dinocyst, terrestrial palynomorphs and foraminifer linings, show a similar trend, with slowly increasing values from the bottom to 3 cm (1999 A.D.), and rapidly increasing values from 3 cm onwards. *Halodinium* and pre-Quaternary palynomorphs fluxes show a quite similar trend with especially, two intervals of increasing fluxes between 28-20 cm and 12-4 cm (1933-1992 A.D.) (Figure 3.6).

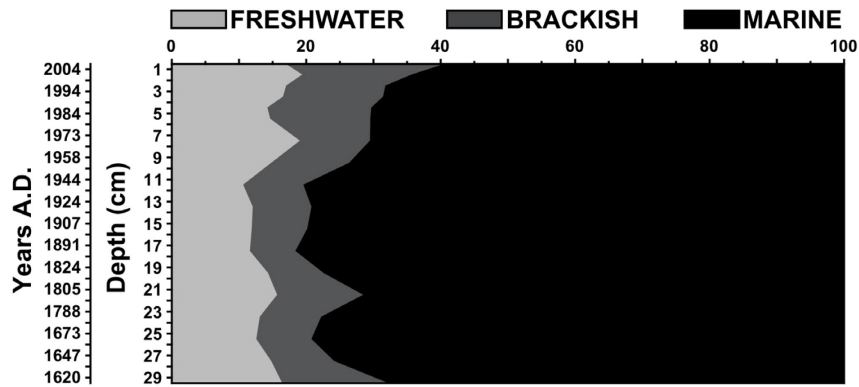
3.4.4. Diatoms

For each core, diatoms show a poor state of preservation and diatom records indicate the dominance of marine taxa accompanied by freshwater and brackish taxa.

NACHVAK 602-1 (59°N)



SAGLEK 617 (58.5°N)



VOISEY'S BAY 624 (56.5°N)

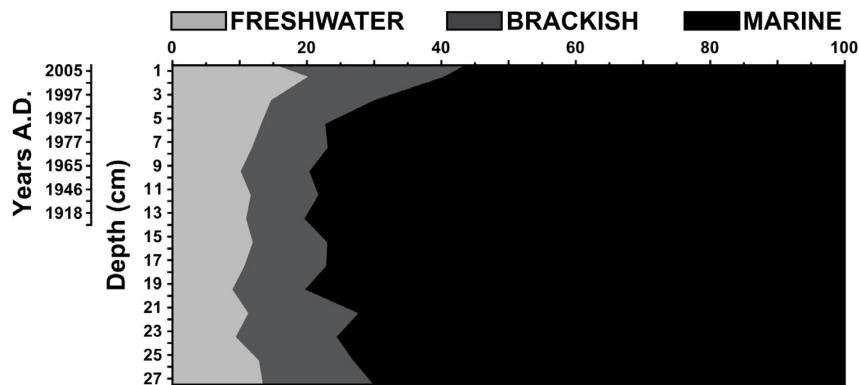


Figure 3.7 : Different water mass influences in the fjords illustrated through diatom relative abundances (%) according to depth (cm) and time (years A.D.).

In N602-1, the abundance of marine taxa ranges from 66% to 76%, while freshwater taxa abundances ranges between 11 and 24% and brackish taxa between 10 and 17% (Figure 3.7). There is little variation of the relative abundance of the diatoms, showing a relative stability of the environment.

In S617, the abundance of marine taxa ranges from 59% to 82%, while freshwater taxa abundances vary between 11 and 19% and brackish taxa between 7 and 24% (Figure 3.7). Between 9 cm and the top of the core (1958-2006 A.D.), we observe an increase of the relative abundance of the diatoms associated with brackish waters.

In V624, the abundance of marine taxa ranges from 56% to 80%, while freshwater and brackish taxa abundances vary between 9 and 20% and 9 and 28%, respectively (Figure 3.7). Between 5 cm and the top of the core (1987-2006 A.D.), we observe an increase of the relative abundance of the diatoms associated with brackish water.

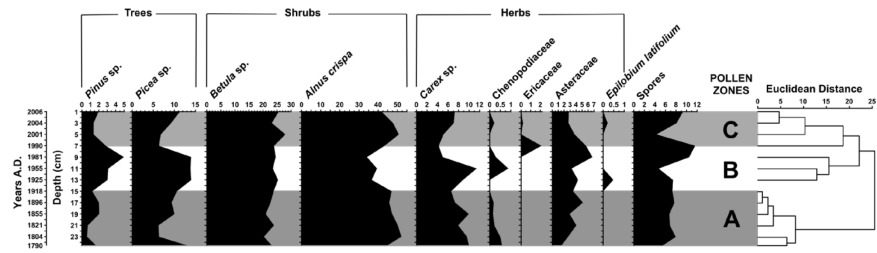
The changes near the top of S617 and V624 cores are associated with a decrease of the abundance of the dominant marine genus *Chaetoceros* sp. and an increase of the brackish genus *Tabellaria* sp. (data not published). This shift in the relative abundance of two genus of diatoms could be explained by a dilution of the water column caused by an input of freshwater, a decrease of the marine water influence or an increase of the turbidity. The latter could be the explanation in V624 because of the increase of sedimentation rate observed also near the top of the core (Figure 3.4). However, considering the poor preservation of the diatoms in the fjords, it is not possible to draw a solid conclusion on the matter.

3.4.5. Pollen and Spore Assemblages

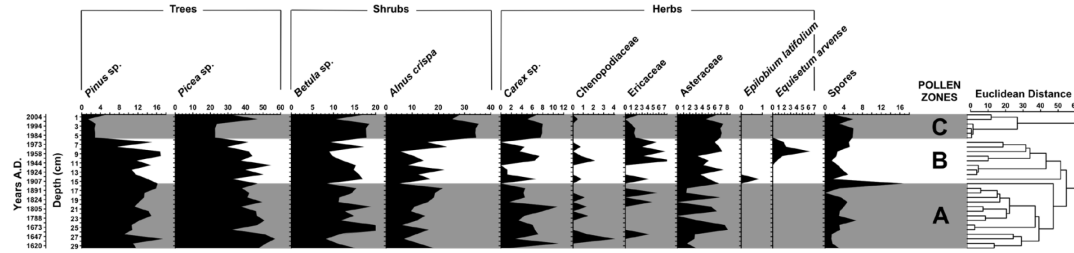
The three fjords show pollen assemblages (Figure 3.8) associated with tundra and forest-tundra landscapes (Lamb, 1984; Fallu et al., 2002; Roberts et al., 2006). Shrub-like trees (*Alnus crispa* and *Betula* sp.) and herb taxa are dominant in the northernmost fjord (Nachvak), while arboreal pollen taxa (*Pinus* sp. and *Picea* sp.) are dominant in the southern studied sites (Saglek and Anaktalak).

In N602-1 three pollen zones can be distinguished. Zone A, at the base of the core (24.5-15 cm) is characterized by the dominance of shrub-like trees such as *Alnus crispa* and *Betula* sp. (average abundance 70%) accompanied by graminoids and herbs (~19%). Zone B, between 15 and 7 cm, marks an increase in the abundance of *Pinus* sp. and *Picea* sp. (+7%). Zone C, from 7 cm to the top of the core, is characterized by the lowest abundance of herbs (~10%) (Figure 3.8).

NACHVAK 602-1 (59°N)



SAGLEK 617 (58.5°N)



VOISEY'S BAY 624 (56.5°N)

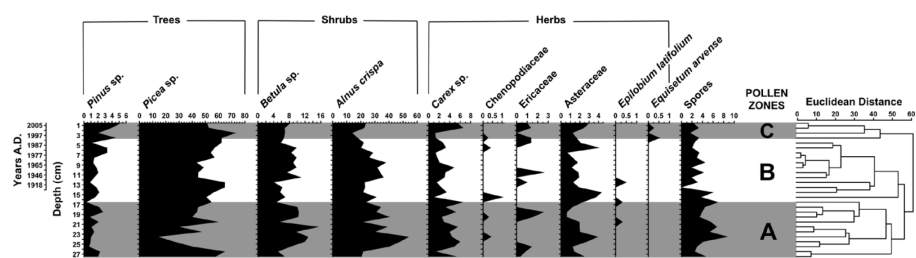


Figure 3.8 : Pollen and spore zones identified from the relative abundances (%) of all the species identified and counted in the three cores, according to depth (cm) and time (years A.D.). Different shades of gray represent pollen zones obtained for each core using a cluster analysis.

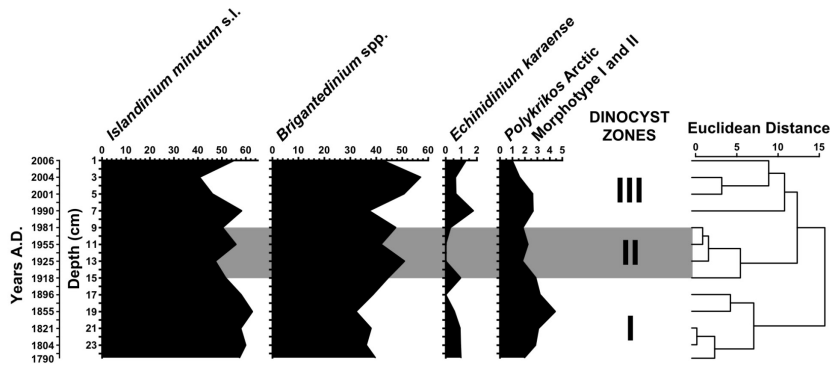
In S617, pollen of coniferous trees are dominant in zone A (29.5-15.5 cm) and B (15.5-5.5 cm) and are gradually replaced in zone C (5.5 cm to the top), which is dominated by shrub-like trees, graminoids and herbs pollen (average abundance 68%). Zone B is differentiated from zone A by an increase in the abundance of herbs (+4%), particularly Ericaceae (+2.5%) and Asteraceae (+1.5%). This core is characterised by the highest abundance of *Pinus* sp. pollen (~11%) (Figure 3.8).

V624 is also characterized by three pollen zones. Zone A (27.5-16.5 cm) shows high abundance of the tree taxa (~45%) but dominance of the shrub-like tree, graminoid and herbs groups (~55%). Zone B (16.5-3.5 cm) marks the increase of the abundance of *Picea* sp. (+10%) and the beginning of the dominance of the coniferous trees group (~55%). Zone C (3.5 cm to the top) marks the highest abundance of coniferous trees pollen (~64%) and the lowest of shrub-like tree (~27%) (Figure 3.8).

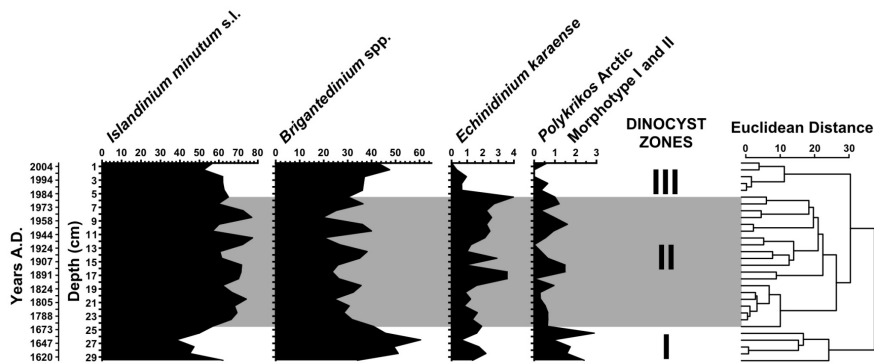
3.4.6. Dinocyst Assemblages

The two northernmost fjords (Nachvak and Saglek) are characterised by low species diversity (n=4) of exclusively heterotrophic dinocyst, while the southernmost fjord (Anaktalak) is characterized by a higher species diversity (n=8) and assemblages dominated by autotrophic taxa (average abundance 95%) (Figure 3.9, Plates 3.1, 3.2).

NACHVAK 602-1 (59°N)



SAGLEK 617 (58.5°N)



VOISEY'S BAY 624 (56.5°N)

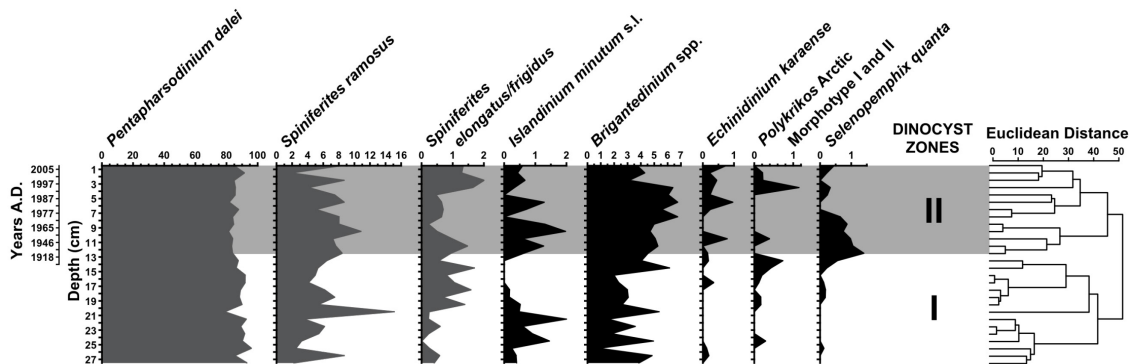


Figure 3.9 : Dinocyst zones identified from the relative abundances (%) of major species identified and counted in the three cores, according to depth (cm) and time (years A.D.). Different shades of gray represent dinocyst zones obtained for each core using a cluster analysis.

In N602-1, we determined three main distinct dinocyst zonation. Assemblage I (25-16 cm) is characterized by the dominance of *Islandinium minutum* s.l. accompanied by maximum abundances of *Polykrikos* Arctic morphotypes I and II. Assemblage II (16-8 cm) is marked by the absence of *Echinidinium karaense* and maximum abundance of *Brigantedinium* spp. Assemblage III (8 cm to the top) is marked by the co-dominance of *Brigantedinium* spp. and *I. minutum* s.l., accompanied by low abundance of *Polykrikos* Arctic morphotypes I and II and *E. karaense*. (Figure 3.9).

In S617, we identified three main dinocyst zones. Assemblage I (30-25 cm) is characterized by the dominance of *Brigantedinium* spp. and minimum abundance of *I. minutum* s.l., accompanied by maximum abundances of *Polykrikos* Arctic morphotypes I and II. Assemblage II (25-5 cm) is characterized by maximum abundances of *I. minutum* s.l. and minimum abundances of *Brigantedinium* spp., accompanied by increasing *E. karaense* and low but persistent *Polykrikos* Arctic morphotypes I and II with decreasing percentages onwards. Finally, assemblage III (5 cm to the top) is marked by the co-dominance of *I. minutum* s.l. and *Brigantedinium* spp., accompanied by minimum abundances of *E. karaense* and *Polykrikos* Arctic morphotypes I and II (Figure 3.9).

We identify two main zonation in core V624. Assemblage I (30-13 cm), is dominated by cysts of *Pentapharsodinium dalei*, accompanied by *Spiniferites ramosus*, *Spiniferites elongatus/frigidus*, *I. minutum* s.l., and *Brigantedinium* spp. Assemblage II (13 cm to the top) is characterized by maximal abundances of *Brigantedinium* spp., *E. karaense* and *Selenopemphix quanta* (Figure 3.9).

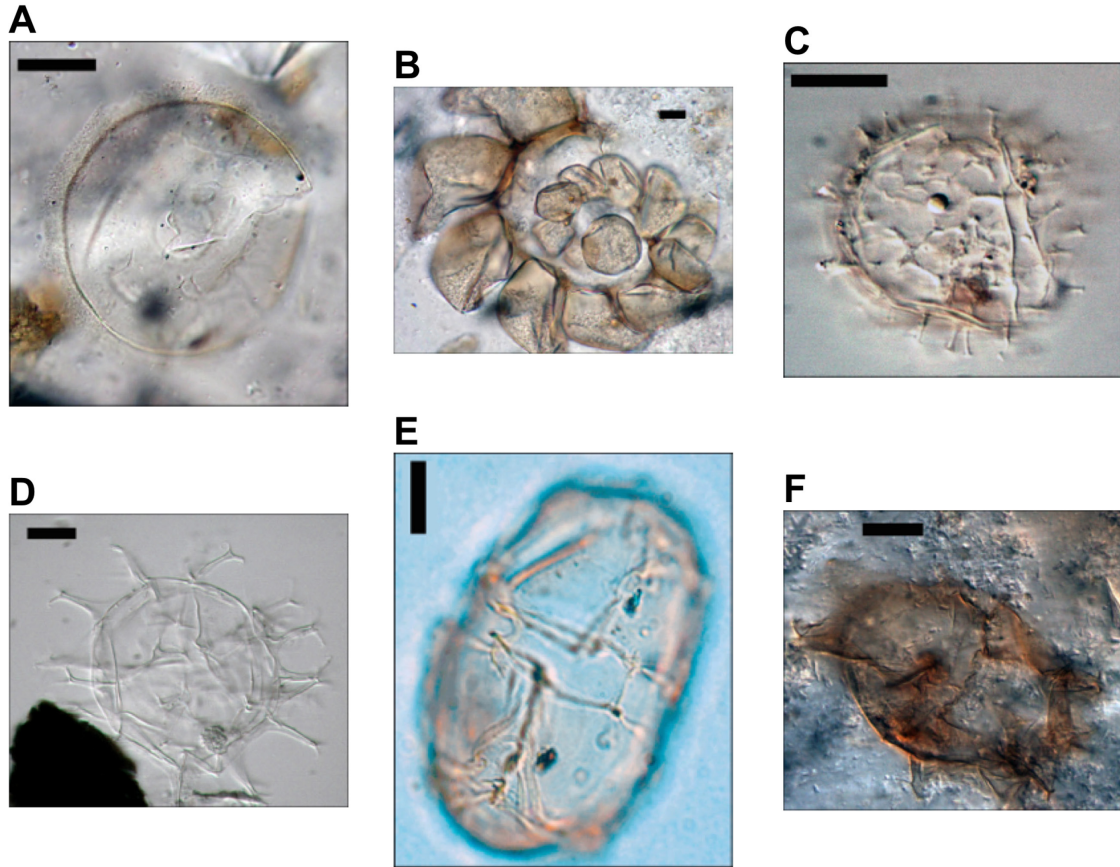


Plate 3.1 : Micrographs of palynomorphs (A and B), and cysts from autotrophic dinoflagellate species (C to F). Each scale bar represents 10 μm ;transmitted-light microscopy at 100 \times magnification. A. *Halodinium* sp., core S617 (11-12 cm). B. Foraminifer lining, core V624 (0-1 cm). C. Cyst of *Pentapharsodinium dalei*, core V624 (23-24 cm). D. *Spiniferites ramosus*, core V624 (23-24 cm). E. *Spiniferites elongatus*, core V624 (17-18 cm). F. *Spiniferites frigidus*, core V624 (14-15 cm).

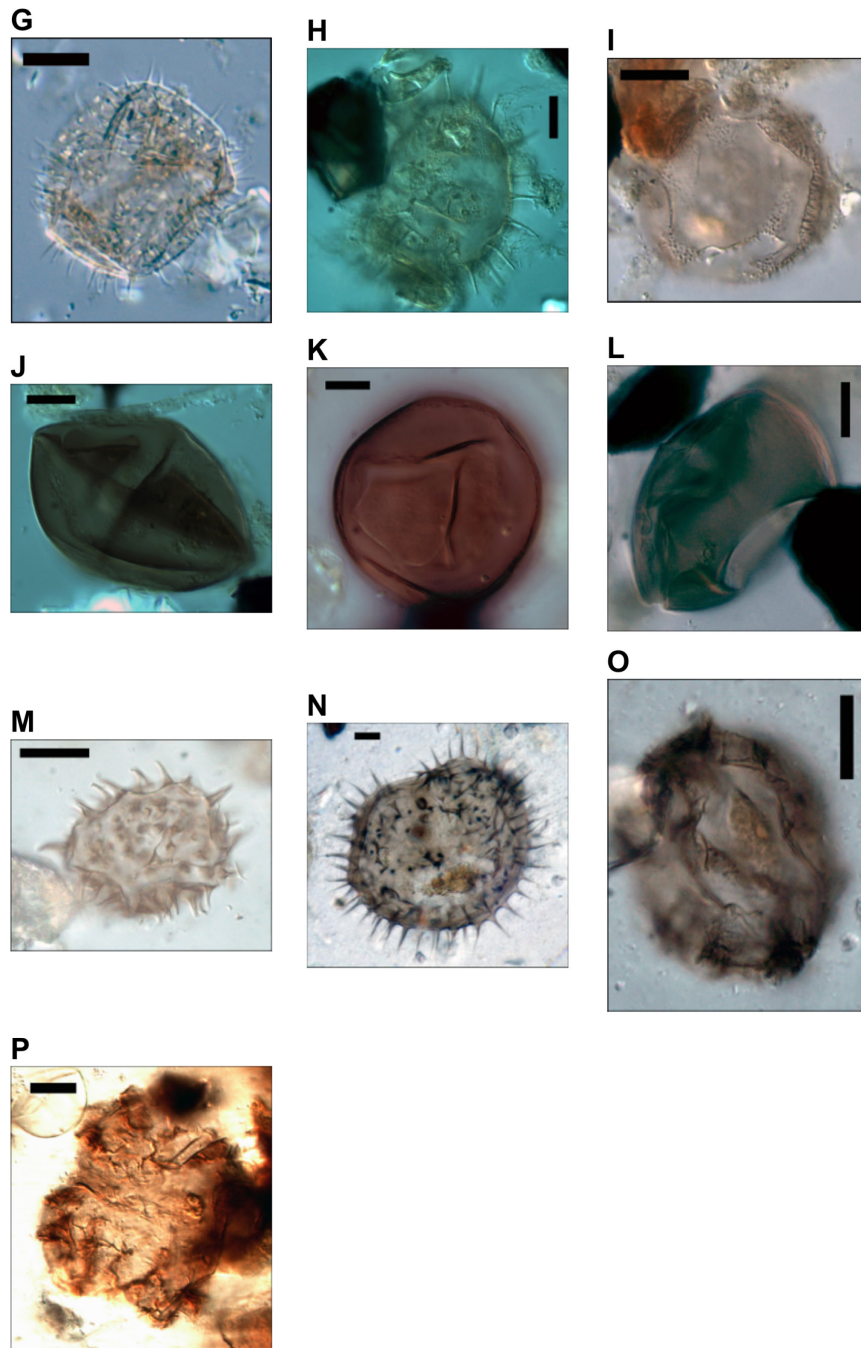
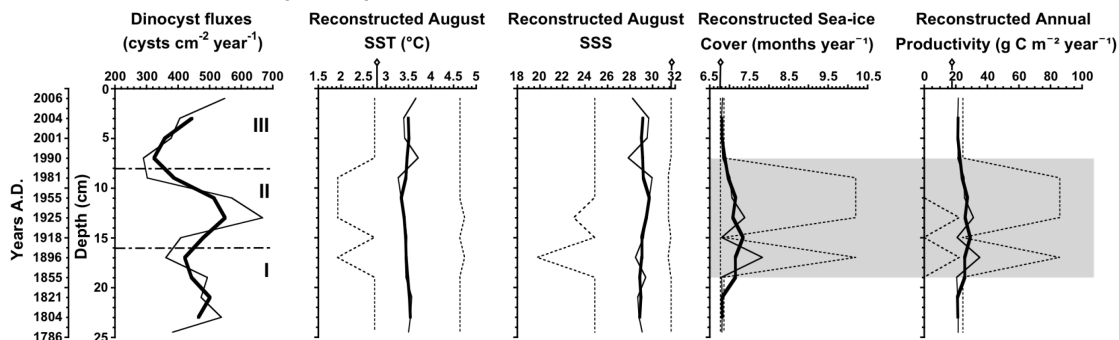


Plate 3.2: Micrographs of cysts from heterotrophic dinoflagellate species. Each scale bar represents 10 μm ; transmitted-light microscopy at 100 \times magnification. G. *Islandinium minutum*, core N602-1 (2-4 cm). H. *Islandinium minutum* var. *cezare*, core N602-1 (10-12 cm). I. *Islandinium brevispinosum*, core N602-1 (6-8 cm). J. *Brigantedinium* sp., core N602-1 (10-12 cm). K. *Brigantedinium simplex*, core N602-1 (10-12 cm). L. *Brigantedinium cariacense*, core N602-1 (10-12 cm). M. *Echinidinium karaense*, core N602-1 (24-25 cm). N. *Selenopemphix quanta*, core V624 (0-1 cm). O. *Polykrikos* Arctic Morphotype I, core S617 (4-5 cm). P. *Polykrikos* Arctic Morphotype II (*quadratus*), core S617 (0-1 cm).

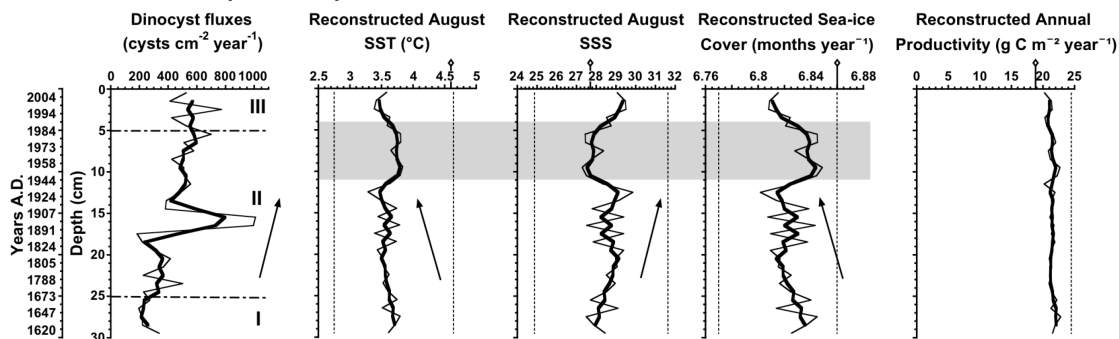
3.4.7. Sea-surface quantitative reconstructions

Sea surface parameter reconstructions based on the Modern Analogue Technique (MAT) are consistent with modern measured values of each parameter (summer temperature and salinity, sea-ice cover duration, productivity (Richerol et al., 2012)), considering the confidence interval for the reconstructions (Figure 3.10). The most salient feature of our reconstructions is the relative stability of the four reconstructed parameters over the last ~220, ~380 and ~130 years, despite some pronounced variations in dinocyst assemblages of cores N602-1, S617 and V624, respectively.

NACHVAK 602-1 (59°N)



SAGLEK 617 (58.5°N)



VOISEY'S BAY 624 (56.5°N)

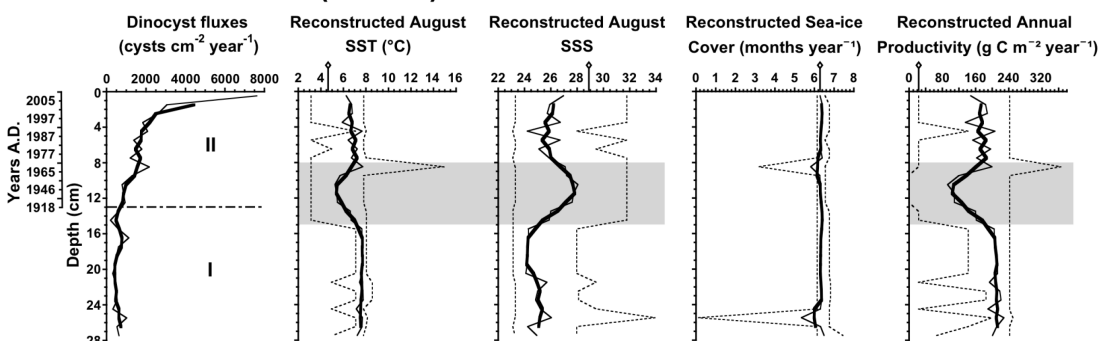


Figure 3.10 : Evolution of dinocyst fluxes (cysts $\text{cm}^{-2} \text{year}^{-1}$) in parallel with the four reconstructed oceanographic parameters, according to depth (cm) and time (years A.D.) : August SST ($^{\circ}\text{C}$), August SSS, Sea-Ice Cover duration (months year^{-1}) and Annual Productivity ($\text{g C m}^{-2} \text{year}^{-1}$). For each curve, the black thick line is a smooth on three values. Horizontal black dotted lines on dinocyst fluxes represent major shift in dinocyst assemblages. Vertical dotted lines represent the confidence interval for each reconstructed parameter at each depth. For each parameter, the black empty diamonds on the x-axis represent modern values. Gray areas highlight the major features presented in the result section. The arrows in S617 illustrate the trends.

In N602-1, reconstructed August SST and SSS remain stable throughout the core. The only noticeable feature is a slight increase of reconstructed sea ice cover duration and annual productivity centered between 1855 and 1990 AD (Figure 3.10). However, these variations are well within the confidence interval for each parameter and are probably not significant.

In S617, reconstructed parameters show subtle changes in their overall trends. Reconstructed August SST and sea ice cover duration both show a general decreasing trend, while reconstructed SSS increases in parallel with dinocyst fluxes (Figure 3.10). All three reconstructed parameters are characterized by a marked shift between 11-4 cm (1944-1989 A.D.), during which SST and sea ice cover increase slightly and SSS decreases (~29.8 to 27.3). Reconstructed productivity remains stable and low (~23 g C m⁻² year⁻¹) throughout the core (Figure 3.10).

In V624, all reconstructed parameters are relatively stable, with the exception of a peak of SST, SSS and productivity between 15 and 8 cm (~1866-1971 A.D.), where both SST and productivity decrease (from 8 to 5°C, and from 200 to 90 g C m⁻² year⁻¹, respectively) and SSS increases (from 24 to 28). Reconstructed sea ice cover remains stable throughout the core (Figure 3.10).

3.5. Discussion

3.5.1. Environmental and anthropogenic history

A fjord is a complex aquatic coastal marine system, resulting from the retreat of a glacier near the coast, and is under the influence of both rivers and ocean (Kahlmeyer, 2011; Bentley and Kahlmeyer, 2012). Previous studies have documented dinocyst and pollen assemblages in sediments from the nearby Labrador Sea (Rochon and de Vernal, 1994; Solignac et al., 2004). Pollen grains showed highest concentrations along the Labrador Shelf with an assemblage composed of species characteristic of the Labrador boreal forest, such as *Picea*, *Alnus* and *Betula*. Higher pollen concentrations reflect the proximity to the source vegetation and are related to both atmospheric and fluvial inputs (Rochon and de Vernal, 1994). Dinocysts assemblages, in previous studies, were dominated by *O. centrocarpum* and *Nematosphaeropsis labyrinthus* accompanied by cysts of *P. dalei* in the Labrador Sea itself and by *Brigantedinium* spp. and *I. minutum* along the Labrador Shelf (Rochon and de Vernal, 1994; Solignac et al., 2004). The dominant taxa were associated with ocean circulation patterns in the Labrador Sea, *O. centrocarpum* with the outer Greenland Current, *N. labyrinthus* with inner East and West Greenland Currents, and *Brigantedinium* spp. and *I. minutum* with the Labrador Current (Rochon and de Vernal, 1994). In our study, palynomorph assemblages in the Labrador Fjords show signs of both important terrestrial and fluvial influences, and a marine influence that is limited to the immediate Labrador Shelf in the two northernmost fjords (Nachvak and Saglek) (Figures 3.8 and 3.9). The dominance of *P. dalei* in the southernmost fjord (Anaktalak) is likely due to a stronger influence of the Labrador Sea or a more productive fjord as illustrated by the highest dinocyst fluxes (Figures 3.6, 3.8, 3.9).

In Nachvak Fjord, the coring site N602 is located deep inside the fjord, far from the marine influence of the Labrador Sea, but not directly under the influence

of a river (figure 3.2A). Analyses of ^{210}Pb for this core reveal a constant sedimentation rate (Figures 3.4 and 3.6). Most of the marine palynomorphs found in our samples behave like silt particles and are subject to the same hydrodynamic constraints as mineral particles (Catto, 1985; Dale, 1996). Grain size analysis of sediments indicates increased proportion of sand of up to 40% from the base to the top of the core (Figure 3.5). This suggests that the area surrounding the coring site is subject to intense bottom current activity and therefore unsuitable for the deposition of fine-grained particles. The oxygenation of bottom waters resulting from such currents could contribute to further decrease the organic matter content of sediments by oxidation. This could explain the progressive decrease of all palynomorphs in the core from bottom to top (Figure 3.6). Freshwater inputs in Nachvak Fjord seem to sustain the planktonic productivity in the water column. A particularly strong freshwater input occurred between ~1918 and 1968 A.D. (~15-10 cm), accompanying a strong increase of both benthic and planktonic productivities (Figure 3.6) and a concomitant peak in the reconstructed sea-ice cover duration and annual productivity (Figure 3.10). Heterotrophic dinoflagellates feed mainly on diatoms (Dale, 1996; Richerol et al., 2012), and during the same period a slight increase in the abundance of freshwater and brackish diatom genera is observed (Figure 3.7). Higher percentages of heterotrophic dinocysts may correspond with episodes of sea-ice expansion (de Vernal et al., 1997). As a consequence of this increase in sea-ice cover, riverine inputs of diatoms from the fjord's watershed may have allowed the increase and dominance of heterotrophic dinoflagellate species. However, the persistent dominance of taxa belonging to the marine-related diatom genus *Chaetoceros*, as well as the presence of dinocysts characteristic of Arctic waters and Labrador Current suggest prevailing marine influence (Figures 3.7 and 3.9; Plate 3.2).

In Saglek Fjord, S617 core was retrieved at the mouth of the fjord, directly under marine influence from the Labrador Sea (Figure 3.2B). All the palynomorph (except terrestrial palynomorph) fluxes show a peak of their respective values between 18-13 cm (1857-1924 A.D.) (Figure 3.6). Pre-Quaternary palynomorph fluxes suggest a more important input of erosive material between ~1857 and

1989 A.D. (18-4 cm), particularly between 1958 and 1989 A.D. (~9-4 cm) (Figure 3.6). *Halodinium* sp. fluxes, although higher after 1924 A.D., resumes its decreasing trend with the exception of some oscillation around 1929 A.D. (12 cm), 1973 A.D. (7 cm) and 1984 A.D. (5 cm), suggesting freshwater inputs (Figure 3.6). These oscillations are consistent with the increase of the proportion of freshwater and brackish diatoms from 9 cm to the top of the core (Figure 3.7). Between ~1929 and 2006 A.D. (12 cm to the top), both dinocyst and foraminifer lining fluxes, respectively, indicate general increases in the planktonic and benthic productivities (Figure 3.6). Between 1950-1986 (~10-5 cm), the marine ecosystem has been contaminated by PCB (PolyChloroBiphenyl) spills from the nearby radar installations belonging to the DEW-Line (Pier et al., 2003; Richerol et al., 2012). The contamination of the bay has apparently been facilitated by increased freshwater runoff transporting detrital material from the watershed. However, as shown by dinocyst assemblages (Figure 3.9) and the dominance of marine diatoms (Figure 3.7), a marine dilution effect likely limited the effects of PCBs on planktonic and benthic productivities (Figure 3.6). The upper 5 cm of the core correspond to the period of decontamination of the military site (1997 to 1999) thereby reducing inputs of contaminated soils and terrestrial erosive materials to the bay area from river and surface water runoff (Richerol et al., 2012) as illustrated by the abrupt decrease of pre-Quaternary palynomorph fluxes (Figure 3.6).

In Anaktalak Fjord, V624 core was retrieved in Voisey's Bay, deep inside the fjord, at the location of a recently installed mining company, not far from Nain which is the northernmost community in Labrador (Figure 3.2C) (Richerol et al., 2012). In this bay, the marine influence ought to be reduced. Between 28-20 cm, *Halodinium* sp. and pre-Quaternary palynomorph fluxes show an increase suggesting an input of erosive material by the river and other freshwater runoff (Figure 3.6). All these changes suggest an important input of terrestrial detrital material into the bay. Between 12-7 cm, an increase of *Halodinium* sp. and pre-Quaternary palynomorph fluxes suggest greater inputs of freshwater and erosive

material into the bay (Figure 3.6). This interval corresponds to the ~1930-1970 A.D. period, which coincides with the final settlement of the northern communities of Labrador (~1959 A.D.) and the more intensive exploitation of the fjord area by the native populations for harvesting and traveling (Rompkey, 2003; McGhee, 2004; Richerol et al., 2012). From 3 cm to the top of the core, palynomorph fluxes (Figure 3.6) as well as freshwater and brackish diatoms (Figure 3.7) show an important increase. These events suggest an increase of the freshwater inputs and thus of terrestrial detrital material into the bay. The increase of the proportion of detrital material during this period (1995-2005 A.D.) was likely caused by the drilling linked to the installation of the Vale Inco Nickel Mine (1997-2002) (Richerol et al., 2012). These digging activities also seem to have favored an increase of planktonic and benthic productivities in the bay. The impact of this digging is also documented by the ^{210}Pb results of the core, which show an important increase of sedimentation rates between 1990 and 2006 A.D. (Figure 3.4).

3.5.2. Climatic history

Elliot and Short (1979) established the tree limit, located between the forest-tundra and the tundra, in Napaktok Bay ($57^{\circ}57'\text{N}$, $62^{\circ}30'\text{W}$), in northern Labrador, between Saglek and Anaktalak fjords (Figure 3.1). Payette (2007) later documented the shifting to the south of this tree limit over the last ~150 years due to the climatic conditions and the influence of the Labrador Current. Nachvak Fjord is located too far north in the tundra zone (Figure 3.1) and has never been affected by this shift over this period, as evidenced by the persistent dominance of pollen from shrub-like trees (*Betula* sp. and *A. crispa*) over pollen from coniferous trees (*Picea* sp. and *Pinus* sp.) (Figure 3.8). The southward shift of the tree limit can be identified more clearly from the Saglek and Anaktalak pollen and spore records. In Saglek, coniferous tree were dominant until 1981 A.D. (~5.5 cm), suggesting forest-tundra conditions (Figure 3.8). The appearance of *Epilobium latifolium* and *Equisetum arvense* pollen in low abundances between 1907-1981 A.D. (pollen

zone B) could reflect a transition towards dryer and colder conditions (Frère Marie-Victorin, 1935; Rousseau, 1974). Hence, the dominance of shrub-like trees is linked to tundra conditions after 1981 A.D. (pollen zone C) (Figure 3.8). In Anaktalak Fjord, the co-dominance of *A. crispa* and *Picea* sp. prior to 1918 A.D. (pollen zone A) suggests a forest-tundra with dryer conditions during this period (Figure 3.8). After 1918 A.D., coniferous pollen predominate in pollen zones B and C, suggesting full forest-tundra conditions (Figure 3.8). Such assemblages indicate a slight cooling of the terrestrial conditions at the beginning of the 20th centuries, resulting in the southward displacement of the tree limit and more prominent tundra conditions around Saglek Fjord.

Most of recent studies of the Arctic and Subarctic regions have documented a warming of the atmospheric conditions and a decrease of sea-ice cover thickness and duration since the beginning of the Industrial Era (ACIA, 2005; Smol et al., 2005; Stroeve et al., 2011; PAGES 2k Consortium, 2013). Few studies in Labrador covered the recent Industrial Era. Paleolimnological studies were carried out on diatom assemblages from the northern Québec-Labrador area, East of Ungava Bay, over the last 100-200 years (Laing et al., 2002; Smol et al., 2005) and from the Saglek Fjord area over the last ~300 years (Gauthier, 2013). Dendroclimatological studies used the latewood density from trees collected around the tree limit in Labrador to discuss summer air temperature on a decadal scale, over the last 350-400 years (D'Arrigo et al., 1996, 2003). The results provided by these studies were in good agreement, showing strong climate stability over northern Labrador, accompanied by a slight cooling trend (D'Arrigo et al., 1996, 2003; Laing et al., 2002; Smol et al., 2005). The study conducted in Saglek Fjord area focused on sediment cores from two lakes with different watershed, ecological and vegetation influences. As a result, fossil diatom assemblages were also different, yet both had the lowest diatom composition turnover for arctic lakes since ~1850 A.D. and did not recorded any significant changes within diatom assemblages over the last ~300 years (Gauthier, 2013). This lack of change in

diatom biodiversity suggested insignificant limnological changes in both lakes over this period and therefore no measurable influence of the recent climate change in the Saglek area compared to other areas of the Arctic and Subarctic where abrupt shifts in aquatic communities have been reported (Douglas et al., 1994; Ponader et al., 2002; Sorvari et al., 2002; Perren et al., 2003; Rühland and Smol, 2005; Solovieva et al., 2005; Perren et al., 2012; Gauthier, 2013). However, more detailed dendroclimatological studies revealed the beginning of a warming trend over the last ~60 years that could be associated with the recent warming recorded over the rest of the Canadian Arctic (D'Arrigo et al., 1996, 2003).

Our reconstructions, based on fossil dinocyst assemblages, concur with these climatic patterns showing the slight climatic cooling over the last ~150-300 years, in particular in Saglek and Anaktalak fjords where reconstructed SST show a slight decrease (Figure 3.10). Our reconstructions are based on a multi-decadal average resolution of the inferred environmental parameters. In fact, at a given site, we are using an average value of a parameter instead of a time series. Thus, the scope of our reconstructions represents a trend over a long time period and has a poor rendition of specific short term events. This explains the absence of the recent warming signal in our reconstructions, as revealed by the tree ring studies of D'Arrigo et al. (1996, 2003). However, the similarity between the overall trends in dinocyst and terrestrial palynomorph fluxes suggests synchronous variations between marine and terrestrial ecosystems. A study by Banfield and Jacobs' (1998) reveals a strong correlation between the winter North Atlantic Oscillation (NAO) index and winter temperature and precipitation in Labrador from 1895 to 1995. During high NAO index winter conditions, Labrador experienced below average winter temperatures and above average winter precipitations. Such a correlation was not found between the summer NAO index and summer temperature and precipitations. However, between ~1895 and 1925 A.D., the winter NAO index was high (Banfield and Jacobs, 1998) and our reconstructions show for the same period a slight decrease in Saglek (~1891-1924 A.D.) and Anaktalak (~1866-1946 A.D.) SST (Figure 3.10). Moreover, this period also coincides with a peak in *Halodinium* sp. in S617, probably due to increased

freshwater inputs related to higher melting of winter snow accumulations (Figure 3.6). In contrast, between 1935 and 1975 the winter NAO index was low (Banfield and Jacobs, 1998) and our SST reconstructions yield almost contemporaneous increases in Saglek (~1935-1958 A.D.) and Anaktalak (~1946-1971 A.D.) (Figure 3.10). In addition, freshwater inputs into Saglek Fjord decreased during this period (Figure 3.6). Thus, it appears that Saglek and Anaktalak fjord climates are influenced by NAO patterns, whereas Nachvak Fjord seems to be more strongly influenced by Arctic systems.

3.6. Conclusions

Sedimentological and palynological analyses conducted on three cores allowed us to document terrestrial and marine influences and to reconstruct the recent history of three subarctic fjords. Station Nachvak 602 is protected from both fully marine and riverine influences, allowing a very good sediment preservation. Cored sites in Saglek and Anaktalak are more subject to the influence of both terrestrial and marine environments as illustrated by higher freshwater inputs and greater dinocyst proportion. In Anaktalak fjord, the recent history and impact of human activities were also noticeable through increases in sedimentation rates and inputs of terrestrial erosive material, reflecting the recent digging activities of a mining company.

As shown in the few previous paleoclimate studies carried out in the northern Labrador region, fossil pollen assemblages and paleoceanographic reconstructions based on fossil dinocyst assemblages recorded in these three fjords also document a strong climate stability of the area with a slight cooling trend. Pollen assemblages from the studied cores indicate cooling of terrestrial conditions as illustrated by the shift of the tree limit to the South during the last ~150 years. Paleoceanographic reconstructions have demonstrated a relative climate stability over the studied period considering the confidence interval of the reconstructions. The two southernmost fjords (Saglek and Anaktalak) also feature a slight cooling trend of SST over the last ~100-150 years and a more pronounced influence of the North Atlantic Oscillation than in Nachvak Fjord.

Acknowledgements

This work was funded through grants from the Natural Sciences and Engineering Research Council of Canada (NSERC) and the Network of Centers of Excellence ArcticNet (project Nunatsiavut) awarded to Reinhard Pienitz and André Rochon, as well as through funding from the Nunatsiavut Government. We wish to thank the officers and crew of the CCGS Amundsen for their help and support during the sampling. We are also grateful to the two anonymous reviewers from the journal *Paleoceanography* who took the time to evaluate our manuscript and gave us very helpful comments.

References

- Arctic Climate Impact Assessment (ACIA), 2005. International Arctic Science Committee (IASC), Cambridge University Press, 1020 pp.
- Arctic Monitoring and Assessment Programme (AMAP), 2011. Snow, Water, Ice and Permafrost in the Arctic (SWIPA): Climate Change and the Cryosphere. AMAP, Oslo, Norway. 538 pp.
- Appleby, P. G. and Oldfield, F., 1983. The assessment of ²¹⁰Pb data from sites with varying sediment accumulation rates. *Hydrobiologia*, 103, 29-35.
- Appleby, P. G., 2001. Chronostratigraphic techniques in recent sediments. In Last, W. M. and Smol, J. P. (Eds) : *Tracking Environmental Change Using Lake Sediments. Volume 1: Basin Analysis, Coring, and Chronological Techniques*. Springer Netherlands, pp171-203.
- Banfield, C. E. and Jacobs, J. D., 1998. Regional patterns of temperature and precipitation for Newfoundland and Labrador during the past century. *The Canadian Geographer*, 42(4), 354-364.
- Bell, T., Josenhans, H., 1997. The seismic record of glaciation in Nachvak Fiord, Northern Labrador. In: Davies, T. A., Bell, T., Cooper, A. K., Josenhans, H., Polyak, L., Solheim, A., Stoker, M. S., Stravers, J. A. (Eds.), *Glaciated Continental Margins: An Atlas of Acoustic Images*. Chapman & Hall, London UK, pp.190-193.
- Bell, T., Dellivers, R. and Edinger, E., 2009. Application of multibeam sonar technology for benthic habitat mapping in Newfoundland and Labrador. *Atlantic Geology*, 45, 1200-1215.
- Bentley, S. J. and Kahlmeyer, E., 2012. Patterns and mechanisms of fluvial sediment flux and accumulation in two subarctic fjords: Nachvak and Saglek Fjords, Nunatsiavut, Canada. *Canadian Journal of Earth Sciences*, 49, 1200-1215.
- Blott, S. and Pye, K., 2001. GRADISTAT: a grain size distribution and statistics package for the analysis of unconsolidated sediments. *Earth Surface Processes and Landforms*, 26(11), 1237-1248.
- Bonnet, S., de Vernal, A., Gersonde, R. and Lembke-Jene, L., 2012. Modern distribution of dinocysts from the North Pacific Ocean (37-64°N, 144°E-148°W) in relation to hydrographic conditions, sea-ice and productivity. *Marine Micropaleontology*, 84-85, 87-113.
- Borcard, D., Gillet, F. and Legendre, P., 2011. Numerical Ecology with R : Chapter 4 – Cluster Analysis. Gentleman, R., Hornik, K. and Parmigiani, G. G. (Eds), *Use R! Series*, Springer, New-York.
- Bouchard, F., Francus, P., Pienitz, R. and Laurion, I., 2011. Sedimentology and geochemistry of thermokarst ponds in discontinuous permafrost, subarctic Quebec, Canada. *Journal of Geophysical Research*, 116, 1-14.
- Campeau, S., Pienitz, R. and Héquette, A., 1999. Diatoms from the Beaufort Sea coast, southern Arctic Ocean (Canada) – Modern analogues for reconstructing Late Quaternary environments and relative sea levels. Lange-Bertalot, H. and Kociolek, P. (Eds), *Bibliotheca Diatomologica* 42, J. Cramer, Berlin-Stuttgart.
- Catto, N. R., 1985. Hydrodynamic distribution of palynomorphs in a fluvial succession, Yukon. *Canadian Journal of Earth Sciences*, 22, 1552-1556.
- Cormier, M.-A., 2013. Étude multi-traceurs de la productivité primaire et du paléoclimat dans le nord de la baie de Baffin. Mémoire de Maîtrise, Université du Québec à Rimouski, Québec Canada, 77 pp.
- Dale, B., 1996. Dinoflagellate cyst ecology : modeling and geological applications. In Jansonius, J. and McGregor, D. G. (Eds) : *Palynology : Principles and Applications*, vol. 3. AASP Found, 1249-1275.

- D'Arrigo, R. D., Cool, E. R. and Jacoby, G. C., 1996. Annual to decadal-scale variations in northwest Atlantic sector temperatures inferred from Labrador tree rings. *Canadian Journal of Forest Research*, 26(1), 143-148.
- D'Arrigo, R. D., Buckley, B., Kaplan, S. and Woollett, J., 2003. Interannual to multidecadal modes of Labrador climate variability inferred from tree rings. *Climate Dynamics*, 20, 219-228.
- de Vernal, A. et Hillaire-Marcel, C., 1987. Paléoenvironnements du Wisconsinien moyen dans l'est du Canada par l'analyse palynologique et isotopique de sédiments océaniques et continentaux. *Revue de Géologie Dynamique et de Géographie Physique*, 27, 119-130.
- de Vernal, A., Bilodeau, G., Hillaire-Marcel, C. and Kassou, N., 1992. Quantitative assessment of carbonate dissolution in marine sediments from foraminifer linings vs. shell ratios; Davis Strait, Northwest North Atlantic. *Geology*, 20(6), 527-530.
- de Vernal, A., Rochon, A., Turon, J.-L. and Matthiessen, J., 1997. Organic-walled dinoflagellate cysts: palynological tracers of sea-surface conditions in middle to high latitude marine environments. *Geobios*, 30, 905-920.
- de Vernal, A., Henry, M., Matthiessen, J., Mudie, P.J., Rochon, A., Boessenkool, K.P., Eynaud, F., Grøsfjeld, K., Guiot, J., Hamel, D., Harland, R., Head, M.J., Kunz-Pirrung, M., Levac, E., Loucheur, V., Peyron, O., Pospelova, V., Radi, T., Turon, J.-L., Voronina, E., 2001. Dinoflagellate cyst assemblages as tracers of sea-surface conditions in the northern North Atlantic, Arctic and sub-Arctic seas : the new 'n=677' data base and its application for quantitative palaeoceanographic reconstruction. *Journal of Quaternary Science* 16(7), 681-698.
- Douglas, M. S. V., Smol, J. P. and Blake, W. J., 1994. Marked post-18th century environmental change in high-arctic ecosystems. *Science*, 266(5184), 416-419.
- Durantou, L., Rochon, A., Ledu, D., Schmidt, S. and Babin, M., 2012. Quantitative reconstruction of sea-surface conditions over the last ~150 yr in the Beaufort Sea based on dinoflagellate cyst assemblages: the role of large-scale atmospheric circulation patterns. *Biogeosciences*, 9, 5391-5406.
- Dutrizac, J. E. and Kuiper, A., 2006. The solubility of calcium sulphate in simulated nickel sulphate-chloride processing solutions. *Hydrometallurgy*, 82, 13-31.
- Elliot, L. T. and Short, S. K., 1979. The northern limit of trees in Labrador: a discussion. *Arctic* 32, 201-206.
- Engstrom, D. R. and Hansen, B. C. S., 1985. Postglacial vegetational change and soil development in southeastern Labrador as inferred from pollen and chemical stratigraphy. *Canadian Journal of Botany*, 63, 543-561.
- Fallu, M.-A., Allaire, N. and Pienitz, R., 2000. Freshwater diatoms from northern Québec and Labrador (Canada) – Species-environment relationships in lakes of boreal forest, forest-tundra and tundra regions. Lange-Bertalot, H. and Kociolek, P. (Eds), *Bibliotheca Diatomologica* 45, J. Cramer, Berlin-Stuttgart.
- Fallu, M.-A., Allaire, N. and Pienitz, R., 2002. Distribution of freshwater diatoms in 64 Labrador (Canada) lakes: species-environment relationship along latitudinal gradients and reconstruction models for water colour and alkalinity. *Canadian Journal of Fisheries and Aquatic Sciences*, 59(2), 329-349.
- Fallu, M.-A., Pienitz, R., Walker, I. R. and Lavoie, M., 2005. Paleolimnology of a shrub-tundra lake and response of aquatic and terrestrial indicators to climatic change in arctic Québec, Canada. *Palaeogeography, Palaeoclimatology, Palaeoecology*, 215, 183-203.

- Fensome, R.A. and Williams, G.L., 2004. The Lentin and Williams index of fossil dinoflagellates. Contribution Series Number 42, American Association of Stratigraphic Palynologists Foundation, Dallas, TX.
- Frère Marie-Victorin, É. C., 1935. Flore Laurentienne. Les Presses de l'Université de Montréal, Montréal (QC) Canada.
- Gauthier, M., 2013. Reconstitution paléolimnologique des conditions environnementales récentes (~300 ans) dans la région de Saglek, Labrador. M.Sc. Thesis, Université du Québec à Chicoutimi (UQAC), Chicoutimi, QC, Canada, 85pp.
- Grimm, E. C., 1987. CONISS: a fortran 77 program for stratigraphically constrained cluster analysis by the method of incremental sum of squares. *Computers and Geosciences*, 13, 13-35.
- Hare, F. K., 1951. Some climatological problems of the Arctic and sub-Arctic. In Malone, T. F. (Ed): *Compendium of Meteorology*. American Meteorological Society, Boston (Massachusetts, USA), 952-964.
- Hare, F. K., 1976. Late Pleistocene and Holocene climates: some persistent problems. *Quaternary Research*, 6, 507-517.
- Head, M.J., Harland, R. and Matthiessen, J., 2001. Cold marine indicators of the late Quaternary : the new dinoflagellate cyst genus *Islandinium* and related morphotypes. *Journal of Quaternary Science*, 16(7), 621-636.
- Heiri, O., Lotter, A.F. and Lemcke, G., 2001. Loss on ignition as a method for estimating organic and carbonate content in sediments : reproducibility and comparability of results. *Journal of Paleolimnology*, 25, 101-110.
- Hulett, L., Dwyer, E., 2003. Voisey's Bay Environmental Assessment Challenges and Successes. PDAC Convention, Toronto, March 2003.
- Intergovernmental Panel on Climate Change (IPCC), 2007. *World Meteorological Organisation*, Cambridge University Press.
- Kahlmeyer, E., 2009. Comparison of the sedimentary record in three sub-arctic fjord systems in northern Labrador. B.Sc. Thesis, Memorial University of Newfoundland, St. John's, NL, Canada. 79 pp.
- Kahlmeyer, E., 2011. Marine records of riverin water and sediment discharge in the fjords of Nunatsiavut. M.Sc. thesis, Memorial University of Newfoundland, St John's NL, Canada, 119 pp.
- Krumbein, W. C. and Pettijohn, F. J., 1938. *Manual of sedimentary petrography*. Appleton-Century-Crofts, New York.
- Laing, T. E., Pienitz, R. and Payette, S., 2002. Evaluation of limnological responses to recent environmental change and caribou activity in the riviere George region, Northern Québec, Canada. *Arctic, Antarctic and Alpine Research*, 34(4), 454-464.
- Lamb, H. F., 1980. Late Quaternary vegetational history of southeastern Labrador. *Arctic and Alpine Research* 12, 117-135.
- Lamb, H. F., 1984. Modern pollen spectra from Labrador and their use in reconstructing Holocene vegetational history. *Journal of Ecology*, 72, 37-59.
- Levac, E. and de Vernal, A., 1997. Postglacial changes of terrestrial and marine environments along the Labrador coast: palynological evidence from cores 91-045-005 and 91-045-006, Cartwright Saddle. *Canadian Journal of Earth Sciences*, 34, 1358-1365.
- McAndrews, J.H., Berti, A. A. and Norris, G., 1973. Key to the Quaternary pollen and spores of the Great Lakes region. Royal Ontario Museum, Toronto, 65 pp.
- McGhee, R., 2004. *The Last Imaginary Place – A Human History of the Arctic World*. Canadian Museum of Civilization, 296 pp.

- Noble, B. F., Bronson, J. E., 2005. Integrating human health into environmental impact assessment : case studies of Canada's Northern Mining Resource Sector. *Arctic* 58(4), 395-405.
- Oldfield, F. and Appleby, P.G., 1984. Empirical testing of ²¹⁰Pb-dating models for lake sediment. In : Haworth, E.Y. and Lund, J.W.G. (Eds) *Lake sediments and environmental history*, p93, University of Minnesota Press.
- PAGES 2k Consortium, 2013. Continental-scale temperature variability during the past two millennia. *Nature Geoscience*, 5, 339-347.
- Payette, S., 2007. Contrasted dynamics of northern Labrador tree lines caused by climate change and migrational lag. *Ecology*, 88(3), 770-780.
- Perren, B. B., Bradley, R. S. and Francus, P., 2003. Rapid lacustrine response to recent High Arctic warming: a diatom record from Sawtooth Lake, Ellesmere Island, Nunavut. *Arctic, Antarctic and Alpine Research*, 35(3), 271-278.
- Perren, B. B., Wolfe, A. P., Cooke, C. A., Kjaer, K. H., Mazzucchi, D. and Steig, E. J., 2012. Twentieth-century warming revives the world's northernmost lake. *Geology*, 40(11), 1003-1006.
- Pier, M. D., Betts-Piper, A. A., Knowlton, C. C., Zeeb, B. A. and Reimer, K. J., 2003. Redistribution of Polychlorinated Biphenyls from a local point source: terrestrial soil, freshwater sediment and vascular plants as indicators of the Halo Effect. *Arctic, Antarctic, and Alpine Research*, 35(3), 349-360.
- Ponader, K., Pienitz, R., Vincent, W.F. and Gajewski, K., 2002. Limnological conditions in a subarctic lake (northern Quebec, Canada) during the late Holocene: analyses based on fossil diatoms. *Journal of Paleolimnology*, 27, 353-366.
- Radi, T. and de Vernal, A., 2008. Dinocysts as proxy of primary productivity in mid-high latitudes of the Northern Hemisphere. *Marine Micropaleontology*, 68(1-2), 84-114.
- Radi, T., Bonnet, S., Cormier, M.-A., de Vernal, A., Durantou, L., Faubert, E., Head, M. J., Henry, M., Pospelova, V., Rochon, A. and Van Nieuwenhove, N., 2013. Operational taxonomy and (paleo-)autoecology of round, brown, spiny dinoflagellate cysts from the Quaternary of high northern latitudes. *Marine Micropaleontology*, 98, 41-57.
- Richerol, T., Rochon, A., Blasco, S., Scott, D. B., Schell, T. M. and Bennett, R. J., 2008a. Distribution of dinoflagellate cysts in surface sediments of the Mackenzie Shelf and Amundsen Gulf, Beaufort Sea (Canada). *Journal of Marine Systems*, 74, 825-839.
- Richerol, T., Rochon, A., Blasco, S., Scott, D. B., Schell, T. M. and Bennett, R. J., 2008b. Evolution of paleo sea-surface conditions over the last 600 years in the Mackenzie Trough, Beaufort Sea (Canada). *Marine Micropaleontology*, 68, 6-20.
- Richerol, T., Pienitz, R. and Rochon, A., 2012. Modern dinoflagellate cyst assemblages in surface sediments of Nunatsiavut fjords (Labrador, Canada). *Marine Micropaleontology*, 88-89, 54-64.
- Roberts, B. A., Simon, N. P. P. and Deering, K. W., 2006. The forest and woodlands of Labrador, Canada: ecology, distribution and future management. *Ecological Research*, 21, 868-880.
- Rochon, A. and de Vernal, A., 1994. Palynomorph distribution in recent sediments from the Labrador Sea. *Canadian Journal of Earth Sciences*, 31, 115-127.
- Rochon, A., de Vernal, A., Turon, J.-L., Matthiessen, J. and Head, M.J., 1999. Distribution of recent dinoflagellate cysts in surface sediments from the North Atlantic Ocean and adjacent seas in relation to sea-surface parameters. *Contribution Series 35, American Association of Stratigraphic Palynologists Foundation : Dallas, TX; 152pp.*
- Rompkey, B., 2003. *The Story of Labrador*. McGill-Queen's University Press, 195 pp.

- Rousseau, C., 1974. Géographie floristique du Québec/Labrador – distribution des principales espèces vasculaires. Les Presses de l'Université Laval, Travaux et Documents du Centre d'Études Nordiques (CEN).
- Rühland, K. and Smol, J. P., 2005. Diatom shifts as evidence for recent Subarctic warming in a remote tundra lake, NWT, Canada. *Palaeogeography, Palaeoclimatology, Palaeoecology*, 226(1-2), 1-16.
- Sawada, M., Gajewski, K., de Vernal, A. and Richard, P., 1999. Comparison of marine and terrestrial Holocene climatic reconstructions from northeastern North America. *Holocene*, 9(3), 267-277.
- Scherer, R. P., 1994. A new method for the determination of absolute abundance of diatoms and other silt-sized sedimentary particles. *Journal of Paleolimnology*, 12(2), 171-179.
- Short, S. K. and Nichols, H., 1977. Holocene pollen diagrams from subarctic Labrador-Ungava : Vegetational history and climatic change. *Arctic and Alpine Research*, 9, 265-290.
- Solignac, S., de Vernal, A. and Hillaire-Marcel, C., 2004. Holocene sea-surface conditions in the North Atlantic – contrasted trends and regimes in the western and eastern sectors (Labrador Sea vs. Iceland Basin). *Quaternary Science Reviews*, 23, 319-334.
- Smol, J. P., Wolfe, A. P., Birks, H. J. B., Douglas, M. S. V., Jones, V. J., Korhola, A., Pienitz, R., Rühland, K., Sorvari, S., Antoniades, D., Brooks, S. J., Fallu, M.-A., Hughes, M., Keatley, B. E., Laing, T. E., Michelutti, N., Nazarova, L., Nyman, M., Paterson, A. M., Perren, B., Quinlan, R., Rautio, M., Saulnier-Talbot, E., Siitonen, S., Solovieva, N. and Weckström, J., 2005. Climate-driven regime shifts in the biological communities of arctic lakes. *Presentation of the National Academy of Sciences of the USA*, 102(12), 4397-4402.
- Solovieva, N., Jones, V. J., Nazarova, L., Brooks, S. J., Birks, H. J. B., Grytnes, J. A., Appleby, P. G., Kauppila, T., Kondratenok, B., Renberg, I. and Ponomarev, V., 2005. Palaeolimnological evidence for recent climatic change in lakes from the northern Urals, Arctic Russia. *Journal of Paleolimnology*, 33(4), 463-482.
- Sorgente, D., Frignani, M., Langone, L. and Ravaioli, M., 1999. Chronology of marine sediments: interpretation of activity-depth profiles of ²¹⁰Pb and other radioactive tracers. *Consiglio Nazionale delle Ricerche, Istituto per la Geologia Marina, Bologna*, 32pp
- Sorvari, S., Korhola, A. and Thompson, R., 2002. Lake diatom response to recent Arctic warming in Finnish Lapland. *Global Change Biology*, 8(2), 171-181.
- Steel, A., Hawboldt, K. and Khan, F., 2009. Analysis of shake flask experiments results conducted on residues from hydrometallurgical processes. *International Journal of Environmental Science and Technology*, 6(1), 57-68.
- Steel, A., Hawboldt, K. and Khan, F., 2010. Assessment of minerals and iron-bearing phases present in hydrometallurgical residues from a nickel sulfide concentrate and availability of residue associated metals. *Hydrometallurgy*, 101, 126-134.
- Stickley, C. E., Koç, N., Brumsack, H.-J., Jordan, R. W. and Suto, I., 2008. A siliceous microfossil view of middle Eocene Arctic paleoenvironments : a window of biosilica production and preservation. *Paleoceanography*, 23, 1-19.
- Stoermer, E. F. and Smol, J. P., 1999. *The Diatoms : applications for the environmental and earth sciences*. Cambridge University Press (UK).
- Stroeve, J. C., Serreze, M. C., Holland, M. M., Kay, J. E., Malanik, J. and Barrett, A. P., 2011. The Arctic's rapidly shrinking sea ice cover: a research synthesis. *Climate Change*, online publication DOI 10.1007/s10584-011-0101-1.

- Stuiver, M., Reimer, P. J. and Reimer, R. W., 2005. CALIB 6.0. <http://calib.qub.ac.uk/calib/>, last access 2013-05-24.
- Viau, A. E. and Gajewski, K., 2009. Reconstructing millennial-scale, regional paleoclimates of boreal Canada during the Holocene. *Journal of Climate*, 22(2), 316-320.
- Vilks, G. and Mudie, P. J., 1983. Evidence for a post-glacial paleoceanographic and paleoclimatic changes in Lake Melville, Labrador, Canada. *Arctic and Alpine Research*, 15, 307-320.
- Wilton, D. H. C., 1996. Mettalogenic overview of the Nain Province, northern Labrador. *CIM Bulletin*, 89, 43-52.
- Zonneveld, K. A. F., Versteegh, G. J. M. and de Lange, G. J., 1997. Preservation of organic-walled dinoflagellate cysts in different oxygen regimes: a 10,000 years natural experiment. *Marine Micropaleontology*, 29, 393-405.
- Zonneveld, K. A. F. and Brummer, G.-J. A., 2000. (Palaeo-)ecological significance, transport and preservation of organic-walled dinoflagellate cysts in the Somali Basin, NW Arabian Sea. *Deep-Sea Research II*, 47, 2229-2256.
- Zonneveld, K. A. F., Versteegh, G. J. M. and de Lange, G. J., 2001. Palaeoproductivity and post-depositional aerobic organic matter decay reflected by dinoflagellate cyst assemblages of the Eastern Mediterranean S1 sapropel. *Marine Geology*, 172, 181-195.